Modeling Psychiatric Disorders Using Patient-derived Induced Pluripotent Stem Cells

By

Ha Nam Nguyen

A dissertation submitted to Johns Hopkins University in conformity with the requirements for the degree of Doctor of Philosophy

Baltimore, Maryland

August 31, 2015

Abstract

Schizophrenia and autism spectrum disorder (ASD) are characterized by complex genetics, variable symptomatology, and anatomically distributed pathology, all of which have made identifying the etiology of these diseases extremely challenging. In addition, our understanding of the role of risk genes in mental disorders has been severely hindered by the lack of access to human neurons. Human induced pluripotent stem cells (iPSCs) derived from patients provide a unique opportunity to investigate the etiology and pathogenesis of these psychiatric disorders. Here, we report the generation and characterization of iPSCs derived from subjects with 15q11.2 copy-number variants (CNVs) and a frameshift mutation in *Disrupted in Schizophrenia 1* (*DISC1*)—both types of mutations are associated with increased risk for schizophrenia and ASD. Mutant iPSCs differentiated toward cortical forebrain lineage revealed dysregulation of neural development and synaptic function. First, iPSC-derived neural progenitors from subjects carrying a 15q11.2 microdeletion exhibit deficits in adherens junctions and apical polarity. This results from haploinsufficiency of *CYFIP1*, a gene within 15q11.2 that encodes a subunit of the WAVE complex, which regulates cytoskeletal dynamics. Second, using isogenic cell lines with and without a specific 4-basepair deletion in *DISC1*, we show that iPSC-derived forebrain neurons with the *DISC1* mutation exhibit functional abnormalities including synaptic transmission deficits and dysregulated expression of many genes related to synaptic function and implicated in psychiatric disorders. Together these iPSC-based investigations of development and function of human neurons demonstrate the capability of this technology for identifying the biological processes and cellular pathways that are impacted by genetic risk for psychiatric disorders.

Thesis advisor: Hongjun Song, Ph.D., Professor, Department of Neurology

Thesis reader: Guo-li Ming, M.D., Ph.D., Professor, Department of Neurology

Preface

I did not know how people get their Ph.D.'s and I certainly did not know much about research. I was lost and about to graduate with a B.S. I did not want to earn a degree that only represents my GPA. I needed a change. So, I delayed my graduation and joined a lab hoping to obtain some skills that could help me find a job in the booming biotech industry in the San Francisco Bay Area. A new path opened up to me and I found a passion for basic biological research. Since, I have worked in several labs, all in academia, and performed many experiments. Every experiment starts with exciting questions and a hint of curiosity; the desire to find the answer and the chance to discover something new have captured my attention and taken me to where I am today. I am about to finish my Ph.D. In this dissertation, I provide a cross-section of my graduate work, two stories published in *Cell Stem Cell* and *Nature*. Thus far, all my work and accomplishments would not be made possible without the teaching, mentoring and support of many people.

I was very fortunate to get acquainted and to have worked with many members of Hongjun Song and Guo-li Ming labs. They are smart, professional, friendly and fun to work with. They make the lab a very welcoming place and a home away from home. I would be a very lucky person if I ever find another lab with a better group of people. To begin, I would like to thank Kim Christian for helping me with the NRSA fellowship application process and many other applications. I would like to extend my gratitude toward my thesis committee members—Linzhao Cheng, Danny Weinberger and Guo-li Ming—for their support and guidance, not only on my projects but also on my career path as well. I also would like to thank my thesis advisor—Hongjun Song. He accepted me into his lab and provided me with everything I needed, including a spacious bench, a

Table of Contents

List of figures

Chapter 1: Introduction

The vast majority of mental disorders, including schizophrenia and autistic spectrum disorder (ASD), are characterized by complex genetics and variable phenotypes. These diseases affect a large number of people across all ethnic groups worldwide. Although there are pharmacological agents available to alleviate some of the symptoms, they often have undesired side effects and are ineffective in a subset of patients[1]. To date, there is no cure for either schizophrenia or ASD and the mechanisms underlying these mental disorders are still mystery. As opposed to monogenic diseases in which a single gene has been identified as a causal factor, these polygenic diseases are associated with multiple risk genes that modulate susceptibility for the disease. Numerous genome-wide studies designed to link genetic variants to complex mental disorders have identified hundreds of risk-associated genes[2-5]. But the investigation of the functional roles of these genes has lagged far behind and has been based on model organisms. Therefore, our knowledge of the biological roles of these risk genes in humans remains limited[6]. To bridge the gap between animal and human models and to work toward a new design for effective therapeutics, it is crucial to develop a better model for understanding how genetic risk factors that contribute to the development, function and regulation of neural systems that are disrupted in the disease state.

Induced pluripotent stem cells (iPSCs) hold significant promise for transforming disease modeling, drug discovery, and regenerative medicine. iPSCs are derived from reprogrammed somatic cells (**Figure 1**); they are similar to embryonic stem cells due to their ability to give rise to all cell types in the body[7]. Because iPSCs retain the genetic information of the donor, they are useful for studying the functional roles of specific risk genes within genetic contexts that are known to be permissive for a given disease. A
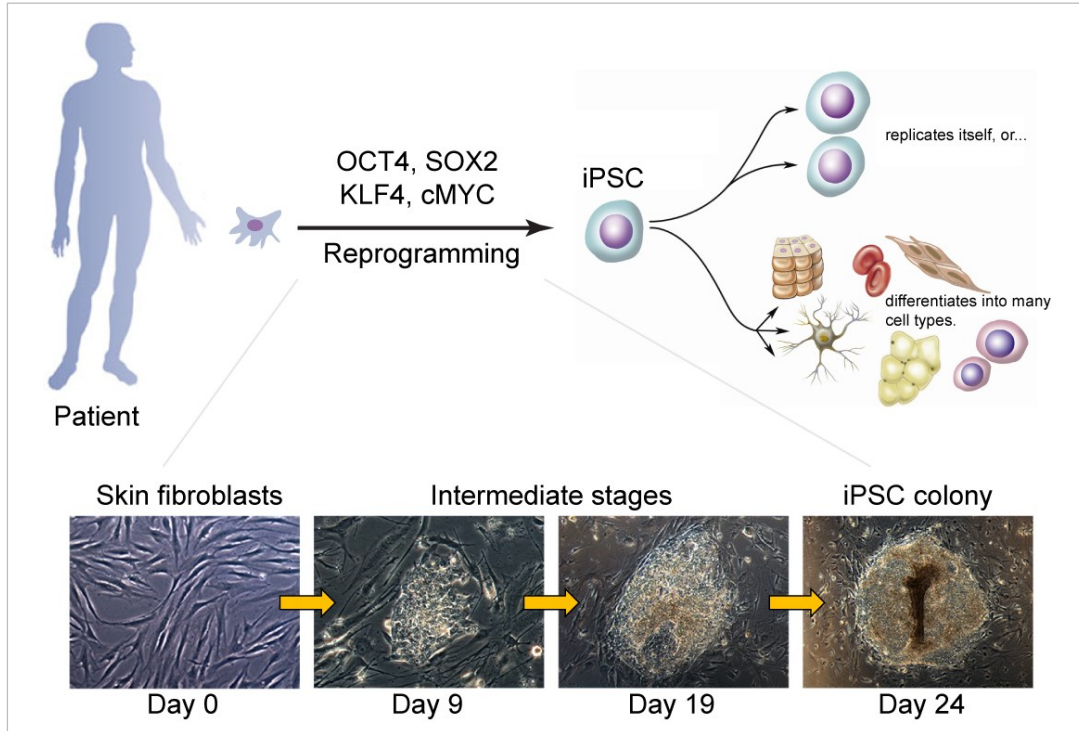
Figure 1. Generation of iPSCs from patients to study mental disorders.

iPSCs are reprogrammed from human-derived fibroblasts by over-expressing the four Yamanaka factors: OCT, SOX2, KLF4 and cMYC. These iPSCs could be maintained indefinitely in culture or differentiated into all cell types in the body.

number of iPSC lines derived from patients with various neurological diseases with complex genetics, including Parkinson's disease, Alzheimer's disease, schizophrenia and autism, have shown that iPSC-derived neurons exhibit some structural and functional phenotypes that respond to the same drug treatments *in vitro* that have been effective in patients[8-13]. However, these studies used iPSCs mainly to validate phenotypes previously identified in animal models or post-mortem brain samples.

Two studies published by Yoon *et al.* (2014) and Wen *et al.* (2014) in *Cell Stem Cell* and *Nature*, respectively, used iPSCs derived from different at-risk populations to model psychiatric disorders[14; 15]. Importantly, these studies established a proof-of-

principle experimental design in which iPSCs were used as a discovery tool to identify new phenotypes and generate novel hypotheses regarding how specific risk genes may contribute to dysregulation of neural development.

In the *Cell Stem Cell* study, I derived and characterized iPSC lines and differentiated them into neuronal lineage. In the *Nature* study, I used a genome editing technology called TALENs to generate multiple isogenic iPSC lines with *DISC1*-4bp mutation. These isogenic iPSC lines served as the basis for determination of the *DISC1* mutation as a causative link for synaptic deficits and dysregulation of genes related to mental disorders that were observed in iPSC-derived forebrain neurons. The full details of the papers are written in Chapter 2 and Chapter 3. Below I provide a preview from each of the papers:

Preview A: Neural stem cells derived from 15q11.2 deletion iPSCs show deficits in adherens junctions and apical polarity

Copy-number variants (CNVs) have emerged as prominent risk factors for various mental disorders such as schizophrenia and autism[16-18]. In particular, 15q11.2 deletion, encompassing *CYFIP1*, *GCP5*, *NIPA1* and *NIPA2*, was identified to have a significant association with schizophrenia. Notably, CYFIP1 has been shown to interact with fragile X mental retardation protein (FMRP) to mediate translation repression and to regulate axonal and dendritic outgrowth[19-21]. The functional roles of others genes in this region are not as clear, especially how they interact to impact risk for schizophrenia. In addition, it is difficult to model CNVs due to their disruption of multiple genes and large DNA regions. For this reason, animal- or cell-based models of 15q11.2 deletion had not been established.

To investigate how 15q11.2 deletion increases risk for schizophrenia, Yoon and colleagues derived iPSCs from three subjects with 15q11.2 deletion. Neuronal progenitor cells (NPCs) differentiated from 15q11.2 deletion iPSCs showed deficits in adherens junctions and apical polarity, early markers of structural integrity. This results from *CYFIP1* haploinsufficiency, which, in turn, negatively affects the WAVE signaling complex. Strikingly, *in vivo* investigation of this phenotype revealed altered migration and ectopic localization of radial glial cells after knockdown of *Cyfip1* during mouse cortical brain development. Building on these results, hypothesis-driven genetic analysis of human post-mortem brain samples identified *ACTR2*, a mediator of CYFIP1 and WAVE signaling complex, as being associated with an increased risk for schizophrenia.

This is the first study to use human iPSCs to investigate 15q11.2 deletion as a prominent risk factor for schizophrenia. It is also the first study to use iPSCs as an entry point to identify a functional role for human CYFIP1, to discover a novel cellular phenotype during human neuronal development, to validate the role of CYFIP1 *in vivo*, and to identify genes that interact with CYFIP1 in human brain samples that may associate with schizophrenia. These findings are consistent with the hypothesis that defects during neural development contribute to psychiatric disorders[22]. However, the functional role of 15q11.2 deletion in mature human neurons remains to be elucidated.

Preview B: Neurons derived from iPSCs with *DISC1* mutation show synaptic dysfunction

The vast majority of psychiatric disorders are characterized by complex genetics and variable phenotypes, all of which have made identifying the etiology of these diseases extremely challenging. The identification of hundreds of risk genes has not itself significantly advanced our understanding of the specific biological and cellular processes

that are dysregulated. Once identified, in depth analyses of individual genes may reveal

vulnerabilities in cellular function that are common to several disorders. One of the most

prominent genetic risk factors is *Disrupted in Schizophrenia 1* (*DISC1*), which was

originally identified at the breakpoint of a balanced chromosomal translocation

(1;11)(q42; q14) that co-segregates with schizophrenia and major mental disorders in a

large Scottish family[23]. Additional association studies revealed that *DISC1* modulates

risk for schizophrenia, bipolar disorder, major depression, and autism[24]. However, due to

different genetic and environmental backgrounds among affected individuals, it is difficult

to determine the impact of *DISC1* mutations in risk for major mental disorders, especially

in the cases of incomplete penetrance.

  To investigate how a mutation in a single gene could lead to an increased risk for

psychiatric disorders, Wen and colleagues derived iPSCs from an American family,

whose members harbor a 4-basepair deletion in *DISC1* and have a history of various

major psychiatric disorders, including schizophrenia[25]. Compared to controls within the

family and outside the family, forebrain neurons derived from patients have deficits in

synaptic vesicle release and dysregulation of many genes related to synapses and

psychiatric disorders. Unexpectedly, they found that mutant DISC1 depletes the wild

type DISC1 in a gain of function manner. To confirm that *DISC1* was responsible for

these deficits, they employed a gene editing technique using transcription activator-like

effector nucleases (TALENs) to generate isogenic iPSCs that differ solely at the 4-bp

deletion locus in *DISC1*. Not only were they able to rescue the deficits in mutant

neurons, but also recapitulated the deficits in control neurons by introducing the mutation

with TALENs. These findings unequivocally demonstrate that mutant DISC1 is a causal

factor for synaptic dysfunction in this iPSC-based model.

Chapter 2

This work entitled "Modeling a risk factor for schizophrenia in iPSCs and mice reveals neural stem cell function associated with adherens junctions and polarity" was published in *Cell Stem Cell* (Volume 15, Issue 1, Pages 79-81) with permission to reprint granted by Elsevier (license # 3667691140503). For simplicity, only the main texts and figures are included; supplemental materials can be accessed online. Below is a graphical abstract associated with the published paper online.
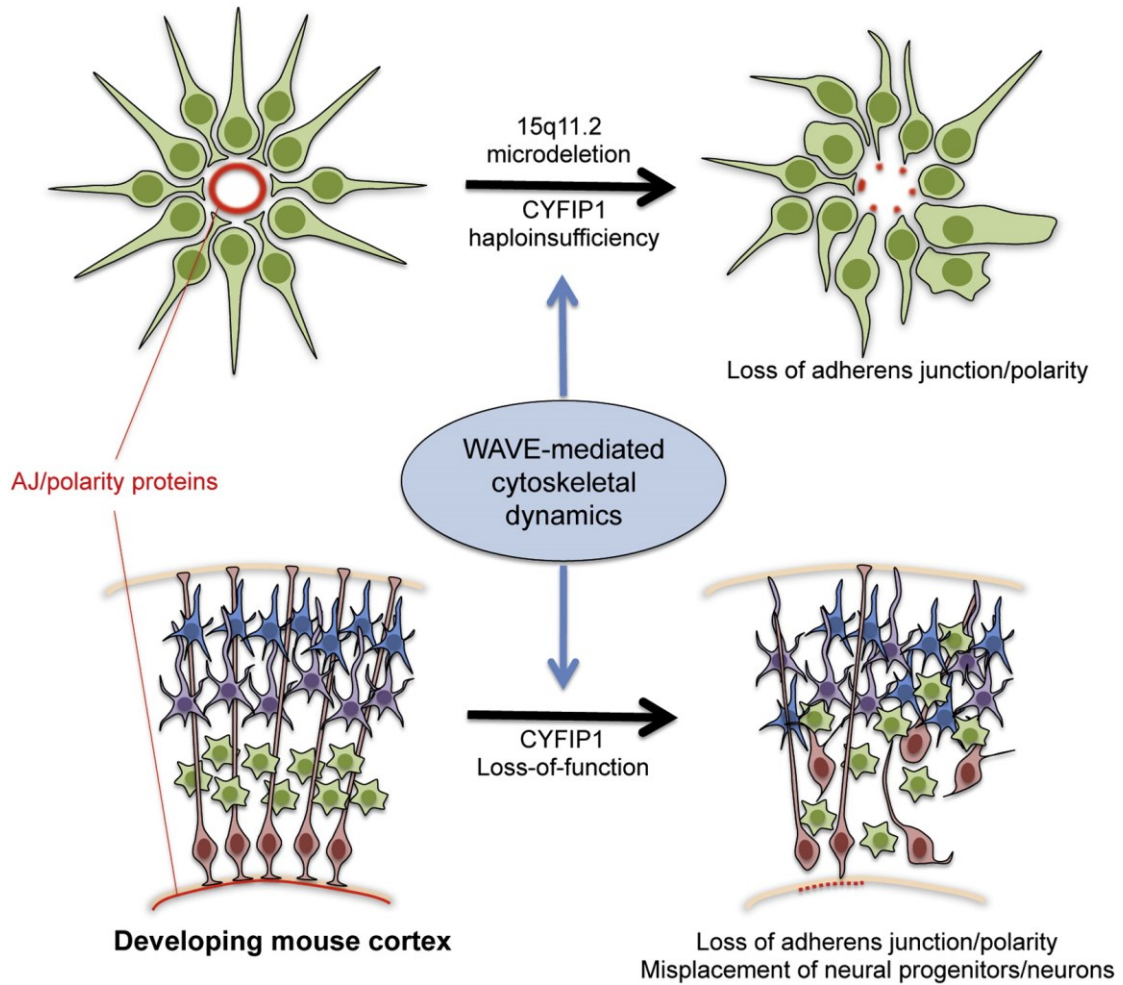
Modeling a risk factor for schizophrenia in iPSCs and mice reveals neural stem cell function associated with adherens junctions and polarity

Ki-Jun Yoon[1,2], Ha Nam Nguyen[1,3], Gianluca Ursini[4], Fengyu Zhang[4], Nam-Shik Kim[1,2], Zhexing Wen[1,2], Georgia Makri[1,2], David Nauen[5], Joo Heon Shin[4], Youngbin Park[1], Raeeun Chung[1], Eva Pekle[1], Ce Zhang[1,2], Maxwell Towe[1], Mohammed Qasim Hussaini S[1], Yohan Lee[6], Dan Rujescu[7], David St. Clair[8], Joel E. Kleinman[4], Thomas M. Hyde[4], Gregory Krauss[2], Kimberly M. Christian[1,2], Judith L. Rapoport[6], Daniel R. Weinberger[2,4,9], Hongjun Song[1,2,3,9#], and Guo-li Ming[1,2,3,9#]

[1]Institute for Cell Engineering, [2]Department of Neurology, [3]Graduate Program in Cellular and Molecular Medicine, [5]Department of Pathology, [9]The Solomon H. Snyder Department of Neuroscience, Johns Hopkins University School of Medicine, Baltimore, Maryland 21205, USA.

[4]Lieber Institute for Brain Development, Johns Hopkins University School of Medicine, Baltimore, Maryland 21205, USA.

[6]Child Psychiatry Branch, National Institute of Mental Health, Bethesda, MD 20892, USA.

[7]Department of Psychiatry, Ludwig-Maximilians University, Munich, Germany.

[8]University of Aberdeen Royal Cornhill Hospital, Aberdeen, UK.

[#] Correspondence should be addressed to:

Guo-li Ming, M.D. & Ph.D.

Institute for Cell Engineering, Johns Hopkins University School of Medicine, 733 N. Broadway, MRB 779, Baltimore, MD 21205, USA; Tel: 443-287-7498

E-mail: gming1@jhmi.edu

Hongjun Song, Ph.D.

Institute for Cell Engineering, Johns Hopkins University School of Medicine, 733 N. Broadway, MRB 759, Baltimore, MD 21205, USA; Tel: 443-287-7499

E-mail: shongju1@jhmi.edu

SUMMARY

Defects in brain development are believed to contribute towards on-set of neuropsychiatric disorders but identifying specific underlying mechanisms has proven difficult. Here, we took a multi-faceted approach to investigate why 15q11.2 copy number variants are prominent risk factors for schizophrenia and autism. First, we show that human iPSC-derived neural progenitors carrying 15q11.2 microdeletion exhibit deficits in adherens junctions and apical polarity. This results from haploinsufficiency of *CYFIP1*, a gene within 15q11.2 that encodes a subunit of the WAVE complex, which regulates cytoskeletal dynamics. In developing mouse cortex, deficiency in CYFIP1 and WAVE signaling similarly affects radial glial cells, leading to their ectopic localization outside of the ventricular zone. Finally, targeted human genetic association analyses revealed an epistatic interaction between CYFIP1 and WAVE signalling mediator ACTR2 and risk for schizophrenia. Our findings provide insight into how CYFIP1 regulates neural stem cell function and may contribute to the susceptibility of neuropsychiatric disorders.

INTRODUCTION

Neuropsychiatric disorders, including schizophrenia and autism, are debilitating

conditions that are postulated to have a neurodevelopmental aetiology (Geschwind,

2009; Weinberger, 1987). Significant progress has been made to identify the genetic

basis of these disorders. In addition to single-nucleotide polymorphisms (SNPs),

submicroscopic variations in DNA copy number (CNVs) are also widespread in human

genomes and specific CNVs have been identified as significant risk factors for

schizophrenia and autism (Malhotra and Sebat, 2012). Because CNVs frequently

contain multiple genes and are more difficult to model in mice using traditional gene

targeting techniques, we know little about how these CNVs affect neural development.

Novel approaches are needed to investigate these genetic risk factors in neural

development and identify their signalling mechanisms, which in turn could generate new

hypotheses for identification of additional risk factors.

15q11.2 CNVs have emerged as prominent risk factors for various

neuropsychiatric disorders, including schizophrenia, autistic spectrum disorder and

intellectual disability (Malhotra and Sebat, 2012). 15q11.2 microdeletion (15q11.2del)

was identified as one of the most frequent CNVs associated with increased risk for

schizophrenia in two large studies (Consortium, 2008; Stefansson et al., 2008), a finding

subsequently confirmed in additional cohorts (Kirov et al., 2009; Tam et al., 2010; Zhao

et al., 2013). Even in normal subjects, 15q11.2del is associated with cognitive variation

and changes in structural measures on MRI scanning (Stefansson et al., 2013). 15q11.2

CNVs encompass four genes, *non-imprinted in Prader/Willi Angelman 1* and *2* (*NIPA1*

and *NIPA2*), *CYFIP1*, and *TUBGCP5* (Figure 1A). While little is known about functions of

these genes in mammalian neural development, CYFIP1 has been shown to interact

with Rac1 (Kobayashi et al., 1998), FMRP (Schenck et al., 2001), and eIF4E (Napoli et al., 2008). Biochemical studies have also identified CYFIP1 as a regulator of the WAVE complex, consisting of WAVE1, WAVE2, Nap1 and Abi1, a complex known to regulate Arp2/3-mediated actin polymerization and membrane protrusion formation in non-neuronal cell lines (Kobayashi et al., 1998; Kunda et al., 2003; Steffen et al., 2004). The function of WAVE signaling in mammalian neurogenesis is not well understood.

Patient-derived induced pluripotent stem cells (iPSCs) provide a new means to investigate how risk factors affect nervous system development (Bellin et al., 2013; Christian et al., 2012). Reprogrammed from somatic cells, iPSCs capture identical risk alleles as the donor individual and provide a renewable resource of previously inaccessible, disease-relevant human cell types to facilitate molecular and cellular investigations. In this emerging new field, recent iPSC studies were mostly "proof-of-principle" experiments that confirmed previous findings from animal and post-mortem human studies; its promise as a discovery tool is just beginning to be realized.

While 15q11.2del is linked to schizophrenia, common variants within the deletion region have not shown similar association in case control studies, possibly because of the weak impact of common SNPs on biological functions of individual genes. To mimic the large dose effect of a whole gene deletion, we hypothesized that genetic interactions within the biological network linked to the function of specific genes within 15q11.2del would rise to the level of clinical association and that patient-derived iPSC studies could provide an entry point to identify these networks (Figure 1B). We established iPSC lines from three individuals carrying 15q11.2del and compared them with iPSCs from five individuals without the CNV. Analysis of iPSC-derived neural rosettes with 15q11.2del revealed impairments in adherens junctions and polarity of human neural progenitor cells (hNPCs) due to WAVE complex destabilization. Pinpointing *CYFIP1-*

haploinsufficiency within 15q11.2 as a underlying cause of hNPC defects then guided our investigation of CYFIP1 and its signaling via the WAVE complex in regulating radial glia neural stem cells (RGCs) in the developing mouse cortex in vivo. This, in turn, led to targeted human genetic association analyses, resulting in the identification of an epistatic interaction for risk of schizophrenia. Our integrated analyses from multiple systems provide novel insight into how 15q11.2 CNVs may contribute to defects in neural development and brain disorders.

RESULTS

Defects in adherens junctions and apical polarity of hNPCs derived from human iPSCs carrying 15q11.2del

To determine how 15q11.2del may affect human brain development, we established multiple iPSC lines from skin fibroblasts of 3 individuals carrying 15q11.2del in one chromosome (Y1, Y3 and Y4) and from 3 control individuals (C1, C2 and C3) using non-integrating approaches (Figure 1C and Table S1). We performed detailed quality control analyses of all iPSC lines selected for the current study (Table S1). These iPSCs maintained embryonic stem cell-like morphology, expressed pluripotency-associated markers and exhibited normal euploid karyotypes (Figures 1C, S1 and Table S1, S2). All iPSC lines tested formed teratomas when injected into SCID mice (Table S1). We also included iPSC lines from two neuropsychiatric patients with a DISC1 mutation as another group for comparison (D2 and D3) (Chiang et al., 2011). Using DNA fluorescence in situ hybridization (FISH), we confirmed one copy microdeletion at 15q11.2 locus in Y1, Y3 and Y4, but not in other fibroblasts and iPSC lines we examined (C1, C2, C3, D2, D3; Figure 1A, D and Table S1).

We first differentiated iPSCs into relatively homogenous primitive neural precursor cells (pNPCs) in monolayer using an established protocol (Li et al., 2011). All lines were efficiently differentiated into pNPCs expressing NESTIN and SOX2 (Figure S2A). No consistent differences in the NPC differentiation efficacy or proliferation among different groups of iPSC lines were detected (Figures S2A-B). To partially maintain cell-cell interaction, we next generated cortical neural rosettes using small molecule inhibitors and retinoic acid (Shi et al., 2012). We initially used 4 iPSC lines for pilot phenotypic characterization, including one iPSC line each from two control subjects (C2-1 and C3-1) and two lines from one subject with 15q11.2del (Y1-1 and Y1-3). Neural rosettes from C2-1 and C3-1 iPSCs showed robust expression of atypical PKCλ, an apical polarity marker, as a ring-like structure at the luminal surface of each rosette (Figure 1E), representing typical formation of apical-basal polarity of hNPCs (Shi et al., 2012). Interestingly, the majority of neural rosettes from Y1-1 and Y1-3 iPSCs exhibited scattered expression of atypical PKCλ (Figure 1E). The structure of adherens junctions as revealed by N-cadherin immunostaining was also disrupted in the majority of rosettes from two Y1-iPSC lines (Figure 1F). These results suggest that gene(s) located within 15q11.2del regulate apical polarity and maintaining adherens junctions of hNPCs.

WAVE complex destabilization and polarity defects of hNPCs due to CYFIP1 haploinsufficiency

The actin cytoskeleton acts as a cytoplasmic anchor for cadherin/catenin proteins at adherens junctions and its proper organization is important for maintaining adherens junctions and polarity of neural precursors in the developing mouse cortex (Buchman and Tsai, 2007). Among the four genes within the 15q11.2 region, CYFIP1 is a regulator of the actin-modulating WAVE complex (Kunda et al., 2003, Steffen et al., 2004, Silva et

al., 2009). Indeed, co-immunoprecipitation (co-IP) analysis showed that CYFIP1 interacts with WAVE complex components WAVE1, WAVE2 and NAP1 (NCKAP1) in normal hNPCs (Figure 2A). Therefore, we assessed WAVE complex integrity in hNPCs derived from different iPSC lines. Consistent with a haploinsufficiency model, mRNAs of all four genes within 15q11.2 were expressed at ~ 50% levels in all hNPCs carrying 15q11.2del compared to those without the deletion (Figure S2C). CYFIP1 protein was also expressed at ~ 50% levels (Figures 2B, 2D and S2D). Strikingly, the expression of WAVE2 protein, but not its mRNA, in 15q11.2del hNPCs was only ~ 20% of that in control hNPCs (Figures 2B, 2E and S2D). The effect of 15q11.2 microdeletion appeared to be specific, as hNPCs derived from mutant DISC1-iPSC lines showed normal expression of CYFIP1 and WAVE2 proteins (Figures 2D-E and S2D). Together, these biochemical analyses demonstrated a specific defect of WAVE complex stabilization in hNPCs with 15q11.2 microdeletion.

Is *CYFIP1* haploinsufficiency the major cause of observed defects in hNPCs carrying 15q11.2del? First, we performed complementation experiments using lentiviruses to increase CYFIP1 levels in two Y1-iPSC lines. We selected two iPSC lines that gave rise to hNPCs with the total amount of CYFIP1 protein at comparable levels to C3-1 hNPCs (Y1-1-CP and Y1-3-CP; Figures 2B, 2D). Importantly, the WAVE2 protein level in these complemented lines was fully rescued (Figures 2B, 2E), suggesting that *CYFIP1* haploinsufficiency is required for WAVE complex destabilization in hNPCs with 15q11.2del. Second, to determine whether decreased CYFIP1 expression is sufficient to cause WAVE complex destabilization in hNPCs, we reduced the endogenous CYFIP1 protein level in control hNPCs to ~ 50% with shRNA (Figure 2C and Table S3). Indeed, expression of shRNA-*CYFIP1*, but not shRNA-control, led to significantly decreased WAVE2 protein expression (Figure 2C). Finally, we examined whether *CYFIP1*

14

haploinsufficiency is the cause of adherens junction and apical polarity impairments observed in neural rosettes from hNPCs with 15q11.2del. We first validated our pilot results using an independent embryoid body protocol (Juopperi et al., 2012), which gave rise to pure PAX6$^+$ neural progenitors (Figure S2E). Scattered expression of atypical PKCλ at the luminal surface was observed for the majority of neural rosettes from multiple iPSC lines with 15q11.2del (Figures 2F-G). Importantly, complementation of CYFIP1 expression to the normal level in two Y1 lines rescued the expression of atypical PKCλ at the luminal surface (Figures 2F-G), whereas reduction of CYFIP1 expression by shRNA in C3-1 hNPCs led to scattered expression of atypical PKCλ (Figure S2F). Consistent with an intact WAVE complex, neural rosettes derived from mutant DISC1-iPSCs exhibited normal distribution of PKCλ at the luminal surface (Figure 2G). Analysis of additional polarity markers, including PAR3 and β-catenin, also showed consistent results across the groups (Figure S2G).

Taken together, this series of biochemical and functional analyses of a collection of 20 iPSC lines established that 15q11.2del, through CYFIP1 deficiency, leads to defects in the maintenance of adherens junctions, apical polarity and WAVE complex stability in hNPCs.

Requirement of CYFIP1 in maintaining adherens junctions and apical polarity of RGCs in developing mouse cortex

Given limitations of in vitro studies of human iPSCs, we next turned to in vivo mouse embryonic cortical development to assess whether the CYFIP1 function we identified in regulating hNPCs is physiologically relevant in vivo and, furthermore, to examine the long-term consequence of CYFIP1 deficiency in cortical development. In the E15.5 dorsal neocortex, CYFIP1 was found to be accumulated at the ventricular surface in the

15

ventricular zone (VZ), with lower expression in migrating neurons in the intermediate zone (IZ; Figure 3A). The VZ of the mid-neurogenic period is mostly occupied by RGCs, which are neural stem cells in the developing cortex (Kriegstein and Alvarez-Buylla, 2009). The apical processes of adjacent RGCs are attached to one another via cadherin-based adherens junctions at the ventricular surface (Loulier et al., 2009; Rasin et al., 2007). Co-immunostaining showed that CYFIP1 was highly expressed at the F-actin-expressing lateral membrane domain, and N-cadherin- and β-catenin-expressing adherens junctions in the apical endfeet of RGCs (Figures 3B-C). With an en face view from the ventricle, CYFIP1 was found as cytosolic puncta inside of the ring-like F-actin structure on the ventricular surface (Figure 3C).

To investigate CYFIP1 function in regulating RGCs, we generated effective shRNAs specifically against mouse *Cyfip1* (Figure S3A and Table S3). We performed in utero electroporation with vectors co-expressing GFP and shRNA-*Cyfip1#2 (*sh-*Cyfip1)*, or control shRNA (sh-control), into the E13.5 neocortex, and analyzed 3 days later. GFP^{+} cells expressing sh-*Cyfip1* showed largely absent CYFIP1 immunoreactivity, confirming the shRNA efficiency against endogenous CYFIP1 in vivo (Figure S3B). While GFP^{+} cells expressing sh-control in the VZ showed robust N-cadherin expression at the ventricular surface, those expressing sh-*Cyfip1* did not (Figures 3D-E). En face view near the ventricular surface further showed reduced N-cadherin expression in some GFP^{-} cells at regions in contact with GFP^{+} cells expressing sh-*Cyfip1*, suggesting a potential non-cell autonomous effect (Figure 3E). Thus, similar to its function in cultured hNPCs, CYFIP1 maintains adherens junctions and apical polarity of neural stem cells in the developing mouse cortex in vivo.

Ectopic localization of CYFIP1-deficient RGCs outside of the VZ

What is the functional consequence of impairments in adherens junctions and apical polarity of RGCs from CYFIP1 deficiency? We examined RGC cell body distribution by Pax6 immunohistochemistry. Pax6$^+$GFP$^+$ cells expressing sh-control were mostly restricted within the VZ (Figures 4A, left panel, and 4B). In contrast, a significant percentage of Pax6$^+$GFP$^+$ cells expressing sh-*Cyfip1* (#2) were ectopically misplaced in the SVZ and IZ, at the expense of VZ localization (Figures 4A, middle panel, and 4B). Aberrant localization of RGCs was also observed with an independent shRNA against mouse *Cyfip1* (#1; Figure S4A). Importantly, this defect was rescued by co-expression of shRNA-resistant CYFIP1 cDNA (Figures 4A, right panel, and 4B), confirming the specificity of shRNA experiments.

GFP$^+$ mitotic cells labeled with phospho-HistoneH3 were also found to be scattered in the SVZ and IZ (Figure 4C). To determine whether NPC proliferation was affected by CYFIP1 deficiency, proliferating cells were pulsed with EdU and examined 2 hours later. Similar to hNPCs in vitro (Figure S2B), CYFIP1-deficient cells showed EdU incorporation comparable to those expressing sh-control, despite their ectopic localization (Figures 4D and S4B). To examine cell cycle progression, we determined the cell cycle exit index defined as the percentage of EdU$^+$Ki67$^-$ cells among all EdU$^+$ cells at 24 hours after EdU administration and did not find any differences (Figure S4C). Together, these results indicate that CYFIP1 is important for proper placement and pattern of mitosis, but not essential for the proliferation and cell cycle progression of RGCs in the developing mouse cortex in vivo.

Ectopic placement of intermediate progenitor cells and cortical neurons generated from CYFIP1-deficient RGCs

We next examined the direct progeny from RGCs, intermediate progenitor cells (IPCs), which express Tbr2 and proliferate transiently in the SVZ to generate neurons (Englund et al., 2005). Tbr2$^+$GFP$^+$ cells expressing sh-*Cyfip1* were also scattered in the VZ/SVZ/IZ, while Tbr2$^+$GFP$^+$ cells expressing sh-control mainly resided in the SVZ (Figures 5A-B). On the other hand, the proportion of Pax6$^+$GFP$^+$ cells and Tbr2$^+$GFP$^+$ cells were not altered between those expressing sh-control and sh-*Cyfip1* (Figure 5C), suggesting that CYFIP1 is dispensable for the proper differentiation of RGCs into IPCs.

Glutamatergic projection neurons of the adult cortex are generated in a stereotyped temporal order, with deep layer neurons (layer V/VI: CTIP2$^+$) produced first and upper layer neurons (layer II/III/IV: Cux1$^+$) produced later (Gaspard et al., 2008; Leone et al., 2008). Defects in RGCs, which serve as the main radial scaffold for migrating neurons, could potentially lead to failure of neurons to reach their normal position. To examine the long-term consequence of *Cyfip1* knockdown on cortical layer formation, we analyzed P5 brains after in utero electroporation of shRNAs at E13.5. CTIP2$^+$ neurons, which normally localize in deeper layers, showed more frequent localization in upper layers after sh-*Cyfip1* expression in RGCs (Figures 5D-E). On the contrary, Cux1$^+$ neurons, which normally localize in upper layers, were present in a higher percentage in deep layers after sh-*Cyfip1* expression (Figures 5D-E). The ratio of CTIP2$^+$ versus CUX1$^+$ cells among all GFP$^+$ cells was not significantly different between sh-control (0.22 $\pm$ 0.03) and sh-*Cyfip1* (0.23 $\pm$ 0.02; n = 4), suggesting that CYFIP1 is dispensable for neuronal subtype specification. Some mis-localized Cux1$^+$ and CTIP2$^+$ cells appeared to be GFP$^-$ (Figure 5D). This could be due to the diluted GFP expression in the P5 brain after multiple rounds of cell division or, alternatively, non-cell autonomous migration defects due to aberrant radial scaffolds of CYFIP1-deficient RGCs. These

results demonstrate that CYFIP1 deficiency causes improper placement of IPCs and glutamatergic projection neurons, resulting in cortical layer malformation.

CYFIP1 signaling mechanism in regulating RGCs in the developing embryonic mouse cortex

Similar to findings from hNPCs (Figure 2A), co-IP analysis using E14.5 mouse cortical lysates showed that endogenous CYFIP1 interacted with several WAVE components, including WAVE1, WAVE2, Abi1 and Nap1 (Figure 6A). Knockdown of CYFIP1 in mouse NPCs in vitro also led to marked decrease of WAVE2 and Abi1 proteins (Figure 6B). Immunohistological analysis showed that WAVE2 protein expression at the ventricular surface was drastically decreased after *Cyfip1* knockdown in vivo (Figure 6C). These results suggested a conserved role and signaling mechanism of CYFIP1 in regulating WAVE complex stability and adherens junctions in both human and mouse NPCs.

Next, we examined the functional role of CYFIP1-dependent WAVE complex and downstream signaling in regulating RGCs in vivo (Figure S5A). We developed effective shRNAs against mouse *Abi1* and downstream mediators *Arp2/3* (Figures S5B-C). In utero electroporation analyses showed a lack of N-cadherin expression at the ventricular surface by GFP⁺ cells expressing sh-*Abi1* or sh-*Arp2/3* (double knockdown; Figure 6D). GFP⁺Pax6⁺ cells expressing sh-*Abi1* or sh-*Arp2/3* also showed scattered distribution in the VZ/SVZ/IZ (Figures 6E-G). These results suggest that, similar to CYFIP1, WAVE complex-mediated signaling is important for the maintenance of adherens junctions and proper placement of RGCs in the developing cortex.

Epistatic interaction of gene expression-associated variants of the WAVE signalling components for risk of schizophrenia

Our findings of similar roles of WAVE signaling components in regulating RGCs,

together with previous findings of association of 15q11.2del with risk for schizophrenia

(Malhotra and Sebat, 2012), led to a new hypothesis that common genetic variants

within the WAVE signalling pathway might interact to affect risk for schizophrenia even in

the absence of association at the individual gene level (Figure 1B). The goal of the

clinical genetic association analyses was to model molecular interactions of CYFIP1 and

WAVE components identified in iPSC and animal studies. We first examined mRNA

expression in the dorso-lateral prefrontal cortex (DLPFC) of post-mortem human brains

in order to find specific genetic variants that were associated with expression of genes in

the WAVE signalling pathway (i.e. expression quantitative trait loci or eQTLs). We

performed a cis-association analysis of SNP variants with gene expression measured by

RNA-seq in a group of 64 Caucasian subjects with no history of medical or psychiatric

disease (Table S4). Significant associations were found for rs268864 with *ACTR2/Arp2*

expression (p = 0.02), rs2797930 with *ABI1* expression (p = 0.02) and rs7168367 with

CYFIP1 expression (p = 0.006). SNP rs4778334, previously associated with risk for

schizophrenia in a case-control Han Chinese sample (Zhao et al., 2013), was also

associated with *CYFIP1* gene expression (p = 0.05). Interestingly, rs4778334 does not

show linkage disequilibrium with other genotyped SNPs in the European ancestry

populations or in the Chinese, consistent with a potential functional effect of this SNP

(Figure S6). We also found that, except for *CYFIP1,* all genes in this network (*ABI1,*

WASF1/WAVE1, WASF2/WAVE2, NCKAP1/Nap1, ACTR2/Arp2 and *ACTR3/Arp3)* tend

to be co-expressed together in a similar pattern (Table S5).

  To search for evidence that eQTLs in the WAVE signalling pathway might be

associated with risk for schizophrenia, we performed single genetic association analysis

of the selected four expression-associated SNPs (or proxy SNPs) in four independent

schizophrenia case-control datasets of European ancestry. No significant single SNP

association was found in any of the four cohorts (Table S6). Targeted pair-wise SNP-

SNP interaction analyses were carried out among three SNPs - rs268864 (SNP1) at

ACTR2, rs4778334 (SNP3) at *CYFIP1||NIPA2* and rs7168367 (SNP4) at *CYFIP1||NIPA1*

as these were only SNPs genotyped in all four cohorts. An interaction was detected

between rs268864 at *ACTR2* and rs4778334 at *CYFIP1||NIPA2* at a marginal

significance (p = 0.0553) in the largest American LIBD/CBDB cohort (Figure 7A). The

same trend of interaction with these exact alleles was also found in three smaller

schizophrenia case-control cohorts of American (GRU; p = 0.147), German (MUN; p =

0.258) and Scottish origin (ABE; p = 0.215). Meta-analysis of the pair-wise interaction in

all four cohorts showed significant evidence for interaction (p = 0.00417) between

rs268864 at *ACTR2* and rs4778334 at *CYFIP1||NIPA2;* interaction analysis of the

combined sample of four cohorts confirmed the interaction in both an additive model (p =

0.0035) and a genotypic model (p = 0.0048; Figure 7A). The results of the meta-analysis

are significant after correction for all combinations of two way interactions based on the

three SNPs analysed. Moreover, the interactions, which were directionally consistent

across all four datasets, were hypothesized based on eQTLs that specifically modelled

the directionality of biologic interactions in the model system experiments.

It is interesting to note that depending on the genotype background of the *ACTR2*

SNP rs268864, genotypes of rs4778334 at *CYFIP1* showed varying effects from

negative to positive on risk of schizophrenia (Figure 7B). In the group of rs268864

genotype AA, individuals carrying genotype CC and CT at rs4778334 were less likely

associated with risk of schizophrenia in comparison with TT genotype (p = 0.0244), and

odds ratio estimates were 0.716 and 0.772 respectively. In contrast, in the group of

rs268864 genotype GG, individuals carrying genotype CC and CT at rs4778334 were

more likely associated with risk of schizophrenia in comparison with TT genotype (p =
0.0103), and odds ratio estimates were 11.14 and 4.56, respectively. Alternating
genotype associations at one locus based on the genotype at another locus are classic
epistatic phenomena.

DISCUSSION

Our study identified the functional role and signalling mechanism underlying CYFIP1
regulation of neural stem cells and provides novel insight into how risk factors for
neuropsychiatric disorders regulate neural development. Using human iPSCs as an
entry point to investigate a prominent CNV risk factor encompassing multiple genes for
schizophrenia and other neuropsychiatric disorders (Figure 1A-B), we uncovered novel
cellular phenotypes in derived hNPCs and identified the responsible gene within the
CNV. These in vitro findings of developmentally relevant phenotypes in human cells
guided our analyses of neural stem cells in the developing mouse cortex in vivo and led
to the identification of the underlying signalling mechanism. The mechanistic insight
allowed us to generate a new hypothesis and test it with gene expression analyses in
human brains and genetic association studies, resulting in the identification of a novel
epistatic interaction for risk of schizophrenia. Our study provides an example of how
genetic risk factors for complex human disorders can be studied in complementary
systems using patient-derived iPSCs as the leading tool for discovery.

      15q11.2 CNVs have emerged as a prominent risk factor for several
neuropsychiatric disorders (Malhotra and Sebat, 2012). Our results from multiple levels
of analyses provide evidence to support a specific gene within this CNV, CYFIP1, as a
potential major contributing factor to biological processes implicated in the
neurodevelopmental origins of these disorders. 15q11.2del has been identified as one of

the three most frequent CNV risk factors for schizophrenia and increases risk 2-4 fold (Consortium, 2008; Stefansson et al., 2008). While none of the SNPs we examined within the CYFIP1 and WAVE signalling pathway showed significant independent risk for schizophrenia in four cohorts of European ancestry, we identified a potential epistatic interaction between *CYFIP1* and WAVE signalling mediator *ACTR2 /Arp2* for increased risk for schizophrenia with an odds ratio up to 11 (Figure 7B). While these results must be taken as preliminary and in need of further replication as the overall statistics are not particularly strong, our study implicates, for the first time, WAVE signalling in risk for schizophrenia and supports an emergent model that multiple factors within the same signalling pathway interact epistatically to affect the risk for psychiatric disorders. Notably, 15q11.2 CNVs themselves are not specific to schizophrenia (De Wolf et al., 2013). In a large study with over 15,000 patient samples, 15q11.2del was found to be strongly associated with developmental delay in children (Cooper et al., 2011). Studies have also linked 15q11.2del to epilepsy (de Kovel et al., 2010; Jahn et al., 2013; Mullen et al., 2013). Interestingly, CNVs with a duplication of this same region have been associated with autistic spectrum disorder (Nishimura et al., 2007; van der Zwaag et al., 2010; Wegiel et al., 2012). In addition, CYFIP1 is within larger 15q11.2-13.1 CNVs that have also been linked to schizophrenia, autistic spectrum disorder, and bipolar disorder (Malhotra and Sebat, 2012). Therefore, our findings have broad implications for these disorders and identify a new signalling pathway for future targeted investigation.

Our study provides novel insight into how CYFIP1 signaling regulates early mammalian neural development. While several previous studies have investigated roles of CYFIP1 in neurons, its function in neural stem cells was completely unknown. In *Drosophila*, the fly ortholog of *Cyfip1* was shown to regulate neuromuscular junction formation (Schenck et al., 2003; Zhao et al., 2013) and eye morphogenesis (Bogdan et

23

al., 2004; Galy et al., 2011). In mice, CYFIP1 interacts with FMRP and cap protein eIF4E to regulate activity-dependent protein translation in mature neurons (Napoli et al., 2008). Furthermore, *Cyfip1* haploinsufficiency in mice produces fragile X-like phenotypes (Bozdagi et al., 2012). By focusing on the earliest stages of cortical development, our study provides evidence for a critical role of CYFIP1 in regulating adherens junctions and apical polarity of both human neural stem cells in the neural rosette model and mouse RGCs in the developing cortex in vivo. Moreover, as a functional consequence of CYFIP1 deficiency, RGCs and their progeny are aberrantly localized in the developing cortex in vivo, resulting in altered stratification of projection neurons and cortical layer malformation. Correct positioning of neurons in the mammalian cortex is a critical determinant of connectivity and neural function, as highlighted by severe neuronal migration disorders in humans (Ross and Walsh, 2001). Deficits in cortical patterning have also been suggested in schizophrenia (Arnold, 1999). A recent study found high incidence of patches of neocortical disorganization in autistic brains (Stoner et al., 2014), reminiscent of what we observed in mouse cortex after in utero exploration to knockdown CYFIP1. Our study therefore provides a new mechanistic model to understand how 15q11.2 CNVs as risk factors may contribute to susceptibility of neuropsychiatric disorders. Our study does not rule out the possibility that other factors within 15q11.2 CNVs affect neural development or that 15q11.2 CNVs also affect functional integrity of mature neurons, as suggested by rodent studies involving eIF4E (Napoli et al., 2008). Future studies of human neurons derived from our iPSC collection will help address the relevance of this pathway in human neuronal function.

Our study also reveals, for the first time, a critical role of the WAVE complex signaling in regulating neural stem cells. Early lethality of knockout mice for the majority of WAVE signaling components, including *CYFIP1* (Bozdagi et al., 2012), *WAVE2*

(Yamazaki et al., 2003; Yan et al., 2003), *Abi1* (Dubielecka et al., 2011), and *Arp3* (Vauti et al., 2007), supports a requisite role of this pathway for mouse survival, which may have precluded in vivo investigation of its role in neural stem cells in early studies. Given that adherens junctions are rapidly lost in newly committed IPCs and neurons (Itoh et al., 2013; Rousso et al., 2012) and that there is little or reduced CYFIP1 expression in IPCs and immature neurons (Figure 3A), our result suggests that aberrant positioning of cortical projection neurons is caused by CYFIP1-WAVE signaling defects in RGCs. Future studies of cell type specific manipulation of CYFIP1-WAVE signaling in IPCs and/or immature neurons will provide a more definitive answer.

Human iPSC technology provides a new experimental platform to investigate cellular phenotypes and mechanisms in genetically tractable and disease-relevant human cell types. To date, patient-derived iPSCs, especially those related to monogenic disorders, have been successfully used to support models of disease pathology developed from animal studies, to demonstrate conserved cellular function of signalling pathways across species, or to facilitate large-scale screening of compounds to identify novel therapeutics (Bellin et al., 2013). Different from monogenic disorders, psychiatric disorders are often genetically complex and typically present with substantial variations in symptoms and degrees of impairment across individuals. Further, many risk associated genetic mutations are not exclusive to clinical populations, nor a particular disease. A key challenge and opportunity for human iPSC biology is to generate new insight into (patho)physiological phenotypes and mechanisms beyond merely supporting previous findings and concepts. Using human iPSCs as a leading discovery tool, we identified novel and consistent cellular phenotypes of neural stem cells that are specific for 15q11.2del, as they were not present in hNPCs derived from iPSCs with a *DISC1* mutation, another risk factor for neuropsychiatric disorders (Thomson et al., 2013). While

genetic risk factors for psychiatric disorders do not code for behaviour, we provide an example that they can lead to specific cellular abnormalities of biological processes implicated in the neurodevelopmental origins of these disorders. Using human iPSCs as an entry point enabled identification of novel investigative targets, followed by validation of in vivo physiological relevance and identification of underlying mechanisms using animal models, and finally, a return to human genetic association studies to support the disease-relevance of the identified pathway in humans (Figure 1B).

In summary, by leveraging and integrating information derived from multiple levels of analyses, ranging from cellular processes in human neural stem cells, in vivo animal models, to targeted human genetic association studies, we provide a novel mechanistic understanding of how 15q11.2 microdeletion affects neural developmental processes. Furthermore, our study illustrates the potential of human iPSC-based research to enable a multifaceted approach to tackle the mystery of complex psychiatric disorders.

EXPERIMENTAL PROCEDURES

iPSC Generation, Culture, Characterization and Neural Differentiation

All iPSC lines were derived from human donor dermal skin fibroblasts using integration-free episomal or Sendai virus methods. Fibroblasts with 15q11.2del (Y1, Y3, and Y4) were collected through the NIMH childhood-onset schizophrenia cohort and their family members (Mattai et al., 2011). All procedures were performed in accordance with IRB and ISCRO protocols approved by the Institutional Committees. iPSCs were cultured and characterized as previously described (Chiang et al., 2011; Juopperi et al., 2012).

iPSCs were differentiated into pNPCs according to a published protocol (Li et al., 2011). Neural rosette formation assays were performed using the mono-layer (Shi et al., 2012) and embryoid body methods (Juopperi et al., 2012). Neural rosettes were initially identified based on polarized pattern of DAPI staining and NESTIN immunoreactivity. Only individual non-overlapped neural rosettes that were 50-200 μm in diameter were included for quantification. The number of rosettes showing an intact apical-ring structure (more than 90% of coverage of apical-ring circumference with atypical PKCλ, N-cadherin, PAR3 or β-catenin immunoreactivity) and incomplete/partial apical structure (less than 90% coverage) were quantified.

In utero Electroporation and Quantitative Analysis of Mouse Cortical Development

in utero electroporation was performed as described (Saito, 2006). For quantitative analysis of electroporated neocortices, GFP$^+$ cells localized within the dorso-lateral cortex were examined. A total of 3–6 brain sections were analyzed per animal by taking 3x3 images to cover the electroporated region of each coronal section with a 25× or 40× objective and comparing them with equivalent sections in littermate counterparts. Quantifications were performed using Imaris software (Bitplane). For distribution plots, the distances between GFP$^+$Pax6$^+$ cells or GFP$^+$Tbr2$^+$ cells and the ventricular surface were calculated by using an in-house MATLAB script (The MathWorks, Inc.), and plotted after dividing each distance by total length of the neocortex and subgrouping into ten equal-size vertical bins (1: the most apical, 10: the most basal).

All animal procedures were performed in accordance with the protocol approved by the Institutional Animal Care and Use Committee.

mRNA Expression Analysis of Post-mortem Human Brains, SNP Genotyping and Clinical Genetic Association and Interaction Analyses

mRNA expression data were generated from post-mortem DLPFC grey matter from 64 subjects without history or diagnosis of a medical or psychiatric disorder (51 males; mean age: 44 ± 14.9 years), all from European ancestry population and matched on age and various post-mortem tissue characteristics. Detailed methods relating to the Brain Tissue Collection of the Clinical Brain Disorders Branch at NIMH (CBDB/NIMH) and the Lieber Institute for Brain Development (LIBD) have been described elsewhere (Colantuoni et al., 2011).

DNA for genotyping was obtained from the cerebella of samples in the collection using Illumina OMNI 2.5M SNP chips. We used ANCOVAs, with age, sex and RIN (RNA Integrity Number) as covariates, to investigate main effects of SNPs on gene expression.

We carried out clinical genetic association and interaction analyses using logistic regression in four independent sample cohorts of cases with schizophrenia and healthy controls. Final interaction analysis was also assessed in the combined sample of four cohorts while controlling cohort effect in order to gain adequate power to detect interactions. The sample collection, genotyping and quality control have been described elsewhere (Zhang et al., 2011).

SUPPLEMENTAL INFORMATION

Supplementary information includes six tables and six figures.

ACKNOWLEDGEMENTS

REFERENCES

Arnold, S. E. (1999). Neurodevelopmental abnormalities in schizophrenia: insights from neuropathology. Dev Psychopathol *11*, 439-456.

Bellin, M., Marchetto, M. C., Gage, F. H., and Mummery, C. L. (2013). Induced pluripotent stem cells: the new patient? Nat Rev Mol Cell Biol *13*, 713-726.

Bogdan, S., Grewe, O., Strunk, M., Mertens, A., and Klambt, C. (2004). Sra-1 interacts with Kette and Wasp and is required for neuronal and bristle development in Drosophila. Development *131*, 3981-3989.

Bozdagi, O., Sakurai, T., Dorr, N., Pilorge, M., Takahashi, N., and Buxbaum, J. D. (2012). Haploinsufficiency of Cyfip1 produces fragile X-like phenotypes in mice. PLoS One *7*, e42422.

Buchman, J. J., and Tsai, L. H. (2007). Spindle regulation in neural precursors of flies and mammals. Nat Rev Neurosci *8*, 89-100.

Chiang, C. H., Su, Y., Wen, Z., Yoritomo, N., Ross, C. A., Margolis, R. L., Song, H., and Ming, G. L. (2011). Integration-free induced pluripotent stem cells derived from schizophrenia patients with a DISC1 mutation. Mol Psychiatry *16*, 358-360.

Christian, K., Song, H., and Ming, G. (2012). Application of reprogrammed patient cells to investigate the etiology of neurological and psychiatric disorders. Frontiers in Biology *7*, 179-188.

Consortium, I. S. (2008). Rare chromosomal deletions and duplications increase risk of schizophrenia. Nature *455*, 237-241.

Cooper, G. M., Coe, B. P., Girirajan, S., Rosenfeld, J. A., Vu, T. H., Baker, C., Williams, C., Stalker, H., Hamid, R., Hannig, V*., et al.* (2011). A copy number variation morbidity map of developmental delay. Nat Genet *43*, 838-846.

de Kovel, C. G., Trucks, H., Helbig, I., Mefford, H. C., Baker, C., Leu, C., Kluck, C., Muhle, H., von Spiczak, S., Ostertag, P*., et al.* (2010). Recurrent microdeletions at 15q11.2 and 16p13.11 predispose to idiopathic generalized epilepsies. Brain *133*, 23-32.

De Wolf, V., Brison, N., Devriendt, K., and Peeters, H. (2013). Genetic counseling for susceptibility loci and neurodevelopmental disorders: the del15q11.2 as an example. Am J Med Genet A *161A*, 2846-2854.

Dubielecka, P. M., Ladwein, K. I., Xiong, X., Migeotte, I., Chorzalska, A., Anderson, K. V., Sawicki, J. A., Rottner, K., Stradal, T. E., and Kotula, L. (2011). Essential role for Abi1 in embryonic survival and WAVE2 complex integrity. Proc Natl Acad Sci U S A *108*, 7022-7027.

Englund, C., Fink, A., Lau, C., Pham, D., Daza, R. A., Bulfone, A., Kowalczyk, T., and Hevner, R. F. (2005). Pax6, Tbr2, and Tbr1 are expressed sequentially by radial glia, intermediate progenitor cells, and postmitotic neurons in developing neocortex. J Neurosci *25*, 247-251.

Galy, A., Schenck, A., Sahin, H. B., Qurashi, A., Sahel, J. A., Diebold, C., and Giangrande, A. (2011). CYFIP dependent actin remodeling controls specific aspects of Drosophila eye morphogenesis. Dev Biol *359*, 37-46.

Geschwind, D. H. (2009). Advances in autism. Annu Rev Med *60*, 367-380.

Itoh, Y., Moriyama, Y., Hasegawa, T., Endo, T. A., Toyoda, T., and Gotoh, Y. (2013). Scratch regulates neuronal migration onset via an epithelial-mesenchymal transition-like mechanism. Nat Neurosci *16*, 416-425.

Jahn, J. A., von Spiczak, S., Muhle, H., Obermeier, T., Franke, A., Mefford, H. C., Stephani, U., and Helbig, I. (2013). Iterative phenotyping of 15q11.2, 15q13.3 and 16p13.11 microdeletion carriers in pediatric epilepsies. Epilepsy Res.

Juopperi, T. A., Kim, W. R., Chiang, C. H., Yu, H., Margolis, R. L., Ross, C. A., Ming, G. L., and Song, H. (2012). Astrocytes generated from patient induced pluripotent stem cells recapitulate features of Huntington's disease patient cells. Mol Brain *5*, 17.

Kirov, G., Grozeva, D., Norton, N., Ivanov, D., Mantripragada, K. K., Holmans, P., Craddock, N., Owen, M. J., and O'Donovan, M. C. (2009). Support for the involvement of large copy number variants in the pathogenesis of schizophrenia. Hum Mol Genet *18*, 1497-1503.

Kobayashi, K., Kuroda, S., Fukata, M., Nakamura, T., Nagase, T., Nomura, N., Matsuura, Y., Yoshida-Kubomura, N., Iwamatsu, A., and Kaibuchi, K. (1998). p140Sra-1 (specifically Rac1-associated protein) is a novel specific target for Rac1 small GTPase. J Biol Chem *273*, 291-295.

Kriegstein, A., and Alvarez-Buylla, A. (2009). The glial nature of embryonic and adult neural stem cells. Annu Rev Neurosci *32*, 149-184.

Kunda, P., Craig, G., Dominguez, V., and Baum, B. (2003). Abi, Sra1, and Kette control the stability and localization of SCAR/WAVE to regulate the formation of actin-based protrusions. Curr Biol *13*, 1867-1875.

Li, W., Sun, W., Zhang, Y., Wei, W., Ambasudhan, R., Xia, P., Talantova, M., Lin, T., Kim, J., Wang, X.*, et al.* (2011). Rapid induction and long-term self-renewal of primitive neural precursors from human embryonic stem cells by small molecule inhibitors. Proc Natl Acad Sci U S A *108*, 8299-8304.

Loulier, K., Lathia, J. D., Marthiens, V., Relucio, J., Mughal, M. R., Tang, S. C., Coksaygan, T., Hall, P. E., Chigurupati, S., Patton, B.*, et al.* (2009). beta1 integrin maintains integrity of the embryonic neocortical stem cell niche. PLoS Biol *7*, e1000176.

Malhotra, D., and Sebat, J. (2012). CNVs: harbingers of a rare variant revolution in psychiatric genetics. Cell *148*, 1223-1241.

Mattai, A. A., Weisinger, B., Greenstein, D., Stidd, R., Clasen, L., Miller, R., Tossell, J. W., Rapoport, J. L., and Gogtay, N. (2011). Normalization of cortical gray matter deficits in nonpsychotic siblings of patients with childhood-onset schizophrenia. J Am Acad Child Adolesc Psychiatry *50*, 697-704.

Mullen, S. A., Carvill, G. L., Bellows, S., Bayly, M. A., Berkovic, S. F., Dibbens, L. M., Scheffer, I. E., and Mefford, H. C. (2013). Copy number variants are frequent in genetic generalized epilepsy with intellectual disability. Neurology *81*, 1507-1514.

Napoli, I., Mercaldo, V., Boyl, P. P., Eleuteri, B., Zalfa, F., De Rubeis, S., Di Marino, D., Mohr, E., Massimi, M., Falconi, M.*, et al.* (2008). The fragile X syndrome protein represses activity-dependent translation through CYFIP1, a new 4E-BP. Cell *134*, 1042-1054.

Nishimura, Y., Martin, C. L., Vazquez-Lopez, A., Spence, S. J., Alvarez-Retuerto, A. I., Sigman, M., Steindler, C., Pellegrini, S., Schanen, N. C., Warren, S. T., and Geschwind, D. H. (2007). Genome-wide expression profiling of lymphoblastoid cell lines distinguishes different forms of autism and reveals shared pathways. Hum Mol Genet *16*, 1682-1698.

Rasin, M. R., Gazula, V. R., Breunig, J. J., Kwan, K. Y., Johnson, M. B., Liu-Chen, S., Li, H. S., Jan, L. Y., Jan, Y. N., Rakic, P., and Sestan, N. (2007). Numb and Numbl are required for maintenance of cadherin-based adhesion and polarity of neural progenitors. Nat Neurosci *10*, 819-827.

Ross, M. E., and Walsh, C. A. (2001). Human brain malformations and their lessons for neuronal migration. Annu Rev Neurosci *24*, 1041-1070.

Rousso, D. L., Pearson, C. A., Gaber, Z. B., Miquelajauregui, A., Li, S., Portera-Cailliau, C., Morrisey, E. E., and Novitch, B. G. (2012). Foxp-mediated suppression of N-cadherin regulates neuroepithelial character and progenitor maintenance in the CNS. Neuron *74*, 314-330.

Schenck, A., Bardoni, B., Langmann, C., Harden, N., Mandel, J. L., and Giangrande, A. (2003). CYFIP/Sra-1 controls neuronal connectivity in Drosophila and links the Rac1 GTPase pathway to the fragile X protein. Neuron *38*, 887-898.

Schenck, A., Bardoni, B., Moro, A., Bagni, C., and Mandel, J. L. (2001). A highly conserved protein family interacting with the fragile X mental retardation protein (FMRP) and displaying selective interactions with FMRP-related proteins FXR1P and FXR2P. Proc Natl Acad Sci U S A *98*, 8844-8849.

Shi, Y., Kirwan, P., Smith, J., Robinson, H. P., and Livesey, F. J. (2012). Human cerebral cortex development from pluripotent stem cells to functional excitatory synapses. Nat Neurosci *15*, 477-486, S471.

Stefansson, H., Meyer-Lindenberg, A., Steinberg, S., Magnusdottir, B. B., Morgen, K., Arnarsdottir, S., and Stefansson, K. (2013). CNVs conferring risk of autism or schizophrenia affect cognition in controls. Nature, doi:10.103/nature12818.

Stefansson, H., Rujescu, D., Cichon, S., Pietilainen, O. P., Ingason, A., Steinberg, S., Fossdal, R., Sigurdsson, E., Sigmundsson, T., Buizer-Voskamp, J. E.*, et al.* (2008). Large recurrent microdeletions associated with schizophrenia. Nature *455*, 232-236.

Steffen, A., Rottner, K., Ehinger, J., Innocenti, M., Scita, G., Wehland, J., and Stradal, T. E. (2004). Sra-1 and Nap1 link Rac to actin assembly driving lamellipodia formation. Embo J *23*, 749-759.

Stoner, R., Chow, M. L., Boyle, M. P., Sunkin, S. M., Mouton, P. R., Roy, S., Wynshaw-Boris, A., Colamarino, S. A., Lein, E. S., and Courchesne, E. (2014). Patches of disorganization in the neocortex of children with autism. N Engl J Med *370*, 1209-1219.

Tam, G. W., van de Lagemaat, L. N., Redon, R., Strathdee, K. E., Croning, M. D., Malloy, M. P., Muir, W. J., Pickard, B. S., Deary, I. J., Blackwood, D. H.*, et al.* (2010). Confirmed rare copy number variants implicate novel genes in schizophrenia. Biochem Soc Trans *38*, 445-451.

Thomson, P. A., Malavasi, E. L., Grunewald, E., Soares, D. C., Borkowska, M., and Millar, J. K. (2013). DISC1 genetics, biology and psychiatric illness. Front Biol (Beijing) *8*, 1-31.

van der Zwaag, B., Staal, W. G., Hochstenbach, R., Poot, M., Spierenburg, H. A., de Jonge, M. V., Verbeek, N. E., van 't Slot, R., van Es, M. A., Staal, F. J.*, et al.* (2010). A co-segregating microduplication of chromosome 15q11.2 pinpoints two risk genes for autism spectrum disorder. Am J Med Genet B Neuropsychiatr Genet *153B*, 960-966.

Vauti, F., Prochnow, B. R., Freese, E., Ramasamy, S. K., Ruiz, P., and Arnold, H. H. (2007). Arp3 is required during preimplantation development of the mouse embryo. FEBS Lett *581*, 5691-5697.

Wegiel, J., Frackowiak, J., Mazur-Kolecka, B., Schanen, N. C., Cook, E. H., Jr., Sigman, M., Brown, W. T., Kuchna, I., Wegiel, J., Nowicki, K.*, et al.* (2012). Abnormal intracellular accumulation and extracellular Abeta deposition in idiopathic and Dup15q11.2-q13 autism spectrum disorders. PLoS One *7*, e35414.

Weinberger, D. R. (1987). Implications of normal brain development for the pathogenesis of schizophrenia. Arch Gen Psychiatry *44*, 660-669.

Yamazaki, D., Suetsugu, S., Miki, H., Kataoka, Y., Nishikawa, S., Fujiwara, T., Yoshida, N., and Takenawa, T. (2003). WAVE2 is required for directed cell migration and cardiovascular development. Nature *424*, 452-456.

Yan, C., Martinez-Quiles, N., Eden, S., Shibata, T., Takeshima, F., Shinkura, R., Fujiwara, Y., Bronson, R., Snapper, S. B., Kirschner, M. W.*, et al.* (2003). WAVE2 deficiency reveals distinct roles in embryogenesis and Rac-mediated actin-based motility. Embo J *22*, 3602-3612.

Zhao, L., Wang, D., Wang, Q., Rodal, A. A., and Zhang, Y. Q. (2013). Drosophila cyfip regulates synaptic development and endocytosis by suppressing filamentous actin assembly. PLoS Genet *9*, e1003450.

Zhao, Q., Li, T., Zhao, X., Huang, K., Wang, T., Li, Z., Ji, J., Zeng, Z., Zhang, Z., Li, K.*, et al.* (2013). Rare CNVs and tag SNPs at 15q11.2 are associated with schizophrenia in the Han Chinese population. Schizophr Bull *39*, 712-719.

FIGURES AND LEGENDS
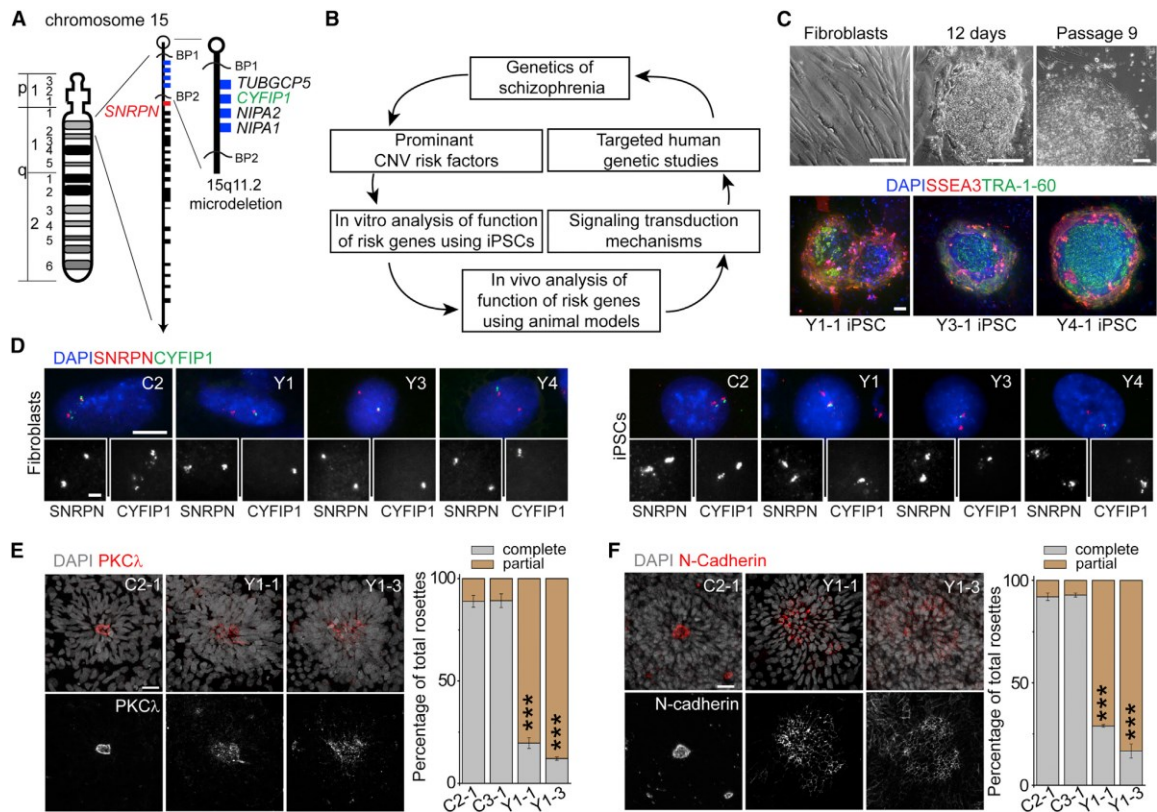
Figure 1. iPSC derivation and aberrant neural rosette formation of hNPCs differentiated from iPSC lines carrying 15q11.2del

(A) An ideogram of Chromosome 15 with proximal 15q11.2 region expanded. Blue boxes indicate the four deleted genes within 15q11.2del, including *CYFIP1*.

(B) A schematic summary of the current study design.

(C) Sample light microscopic images and fluorescent images of fibroblasts and iPSC colonies for immunostaining of pluripotency markers. Scale bars, 100 μm.

(D) Sample fluorescence in situ hybridization (FISH) images of donor fibroblasts and derived iPSC lines. Two FISH probes, one for *CYFIP1* locus and one for *SNRPN* locus (outside of 15q11.2; See A for the genomic location), were used. Scale bar, 10 μm.

(E-F) Defects in adherens junctions and apical polarity of hNPCs derived from iPSCs with 15q11.2del. Shown on the left are sample confocal images of immunostaining of atypical PKCλ (E) and N-cadherin (F) for neural rosettes differentiated from iPSCs by the mono-layer method. Scale bars, 20 μm. Shown on the right are quantifications of neural rosettes with complete "apical ring-like structure" ($\geq$ 90% coverage of apical-ring circumference with atypical PKCλ or N-cadherin immunoreactivity) or "partial/scattered" (< 90% coverage). Values represent mean $\pm$ SEM (n = 3 cultures; ***p < 0.001; Student's t-test).

See also Figures S1, S2 and Tables S1, S2.
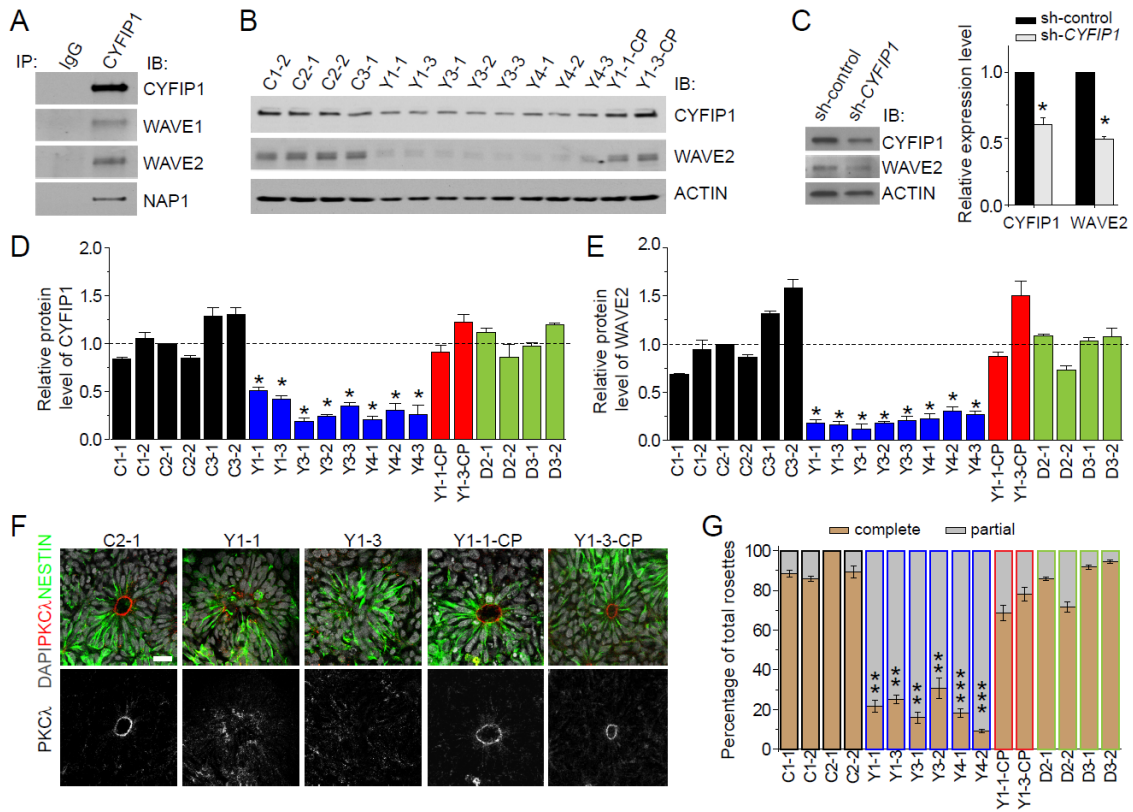
Figure 2. Destabilization of the WAVE complex and polarity defects of hNPCs due to CYFIP1 deficiency

(A) CYFIP1 is a component of WAVE complex in human pNPCs. Shown are sample Western blot images of co-IP analysis of pNPCs using anti-CYFIP1 antibodies.

(B) Reduced CYFIP1 and WAVE2 protein levels in pNPCs carrying 15q11.2del. Lentiviruses were used to establish two CYFIP1 complementation lines (Y1-1-CP and Y1-3-CP).

(C) Decreased WAVE2 protein levels after CYFIP1 knockdown by lentivirus-mediated shRNA expression in normal pNPCs for 48 hrs.

(D-E) Quantification of protein levels of CYFIP1 and WAVE2 among different pNPCs. All data were normalized to ACTIN levels for loading control and then normalized to CYFIP1

(D) or WAVE2 (E) in C2-1 pNPCs for comparison. Values represent mean $\pm$ SEM (n = 3-5 cultures; *p < 0.05; Student's t-test).

(F-G) Defect in adherens junction and apical polarity of hNPCs carrying 15q11.2del and its rescue by CYFIP1 complementation. Shown on the left are sample confocal images of immunostaining of atypical PKCλ for neural rosettes differentiated from iPSCs using the embryoid body method. Scale bar, 20 μm. Shown on the right are quantifications of neural rosettes similar as in Figure 1E. Values represent mean $\pm$ SEM (n = 5 cultures; ***p < 0.001; **p < 0.01; Student's t-test).

See also Figure S2 and Tables S1, S3.
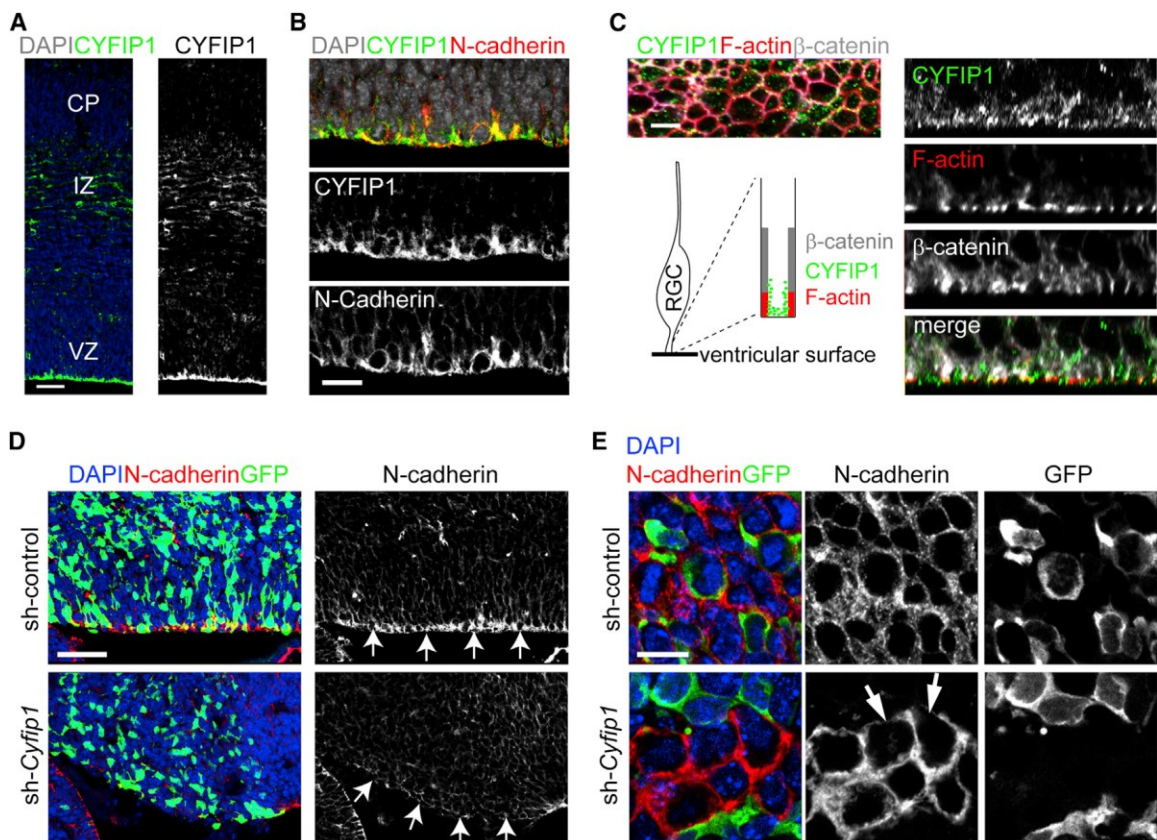
Figure 3. Critical role of CYFIP1 in regulating adherens junctions and apical polarity of RGCs in the developing mouse cortex

(A-C) Expression of CYFIP1 in the mouse neocortex at E15.5. Shown are sample

confocal images of immunostaining of CYFIP1 and N-cadherin. VZ: ventricular zone; IZ:

intermediate zone; CP: cortical plate. Also shown is the en face view of CYFIP1

expression at the ventricular surface (C, left panel). The structure of F-actin, which forms

the boundary between apical endfeet of RGCs on the ventricular surface, was labelled

by Phalloidin-Alexa594 (Red). Cross-section images are shown in right panels. Scale

bars, 50 μm (A), 20 μm (B) and 5 μm (C).

(D-E) Expression of CYFIP1 and other apically polarized proteins in the mouse

neocortex at E16.5 after in utero electroporation at E13.5 to co-express GFP and sh-

control or sh-*Cyfip1* (#2). Shown are sample confocal images of immunostaining for GFP

and N-cadherin (D) and the en face view at 3 μm from the ventricular surface (E). Scale

bars: 50 μm (D) and 10 μm (E).

See also Figure S3 and Tables S2, S3.
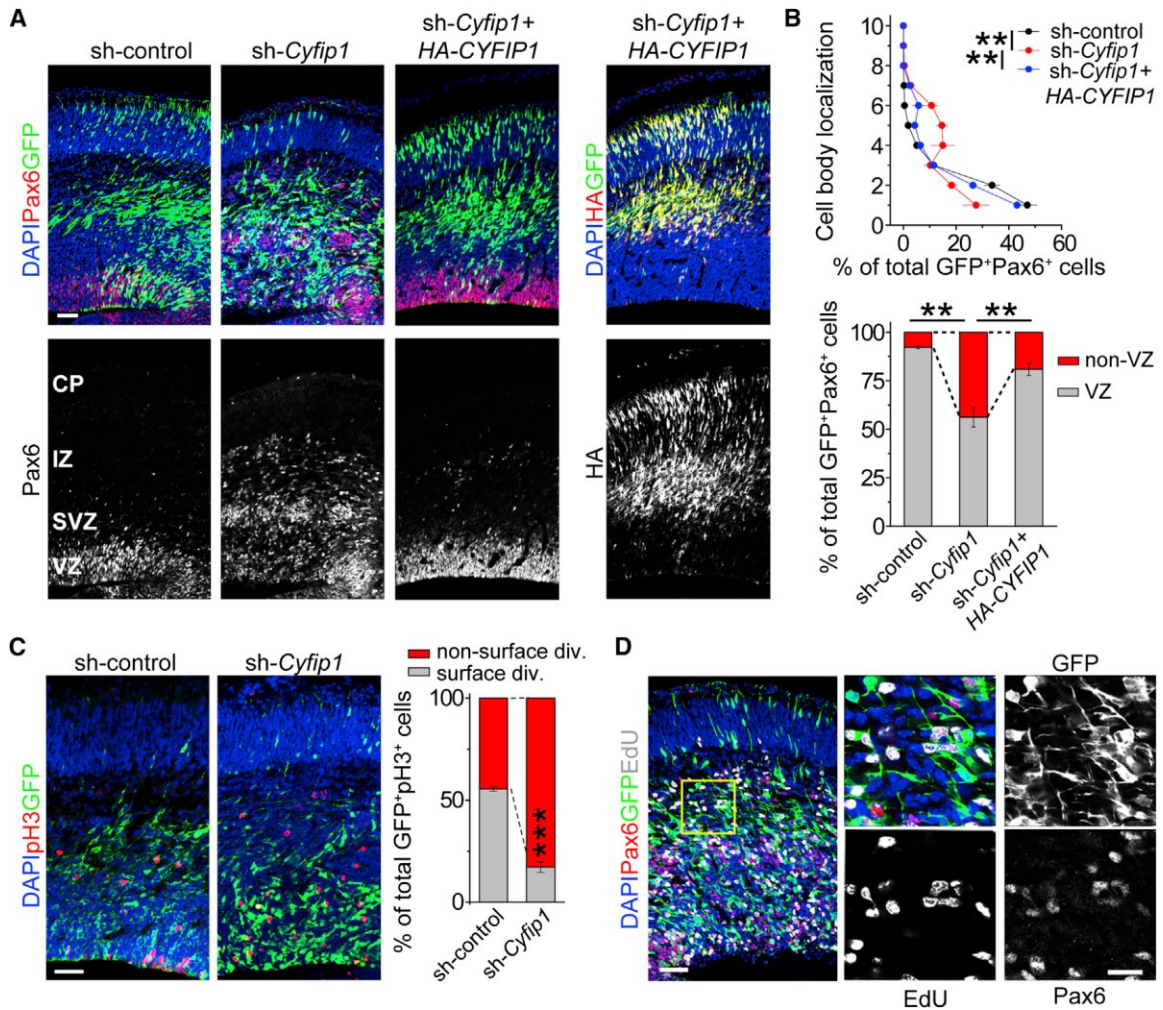
Figure 4. Ectopic localization of CYFIP1-deficient RGCs outside of the VZ in the developing mouse cortex

(A-B) Ectopic localization of Pax6+ RGCs in the SVZ and IZ of E16.5 neurocortices after in utero electroporation at E13.5 to co-express GFP and sh-control or sh-*Cyfip1*, or co-express GFP/sh-*Cyfip1* and cDNA for shRNA-*Cyfip1* resistant HA-tagged CYFIP1. Shown in (A) are sample confocal images of immunostaining of Pax6, GFP and HA. Co-transfection of GFP/sh-*Cyfip1* and shRNA-resistant HA-tagged CYFIP1 was confirmed by co-localization of GFP and HA immunostaining (the right-most panel). Scale bar, 50 μm. Shown in (B) are two different quantifications of the distribution of GFP+Pax6+ cells

in the neocortex. Upper panel represents GFP$^+$Pax6$^+$ cells in each of ten equal-size

vertical bins expressed as percentages of total GFP$^+$Pax6$^+$ cells (1: the most apical, 10:

the most basal). Lower panel represents percentages of GFP$^+$Pax6$^+$ cells in the VZ (VZ)

and in other layers (non-VZ). Values represent mean $\pm$ SEM (n = 4-5 animals; **p <

0.01; Student's t-test).

(C) Aberrant localization of proliferating cells expressing sh-*Cyfip1* in E16.5 neocortex.

Sample confocal images of immunostaining for GFP and an M-phase marker, phospho-

HistoneH3 (pH3), are shown. Scale bar, 50 μm. Also shown are quantifications of

percentages of GFP$^+$pH3$^+$ cells at the ventricular surface (surface division) and at other

locations (non-surface division). Values represent mean $\pm$ SEM (n = 5 animals; ***p <

0.001; Student's t-test)

(D) Proliferation of CYFIP1-deficient RGCs outside of the VZ. E13.5 embryos were

electroporated to co-express GFP and sh-*Cyfip1* and fixed at 2 hrs after EdU injection at

E16.5. Shown are sample confocal images of staining for GFP, Pax6, EdU and DAPI.

Note that ectopic GFP$^+$Pax6$^+$ cells in the IZ still incorporated EdU, representing their

ability to proliferate far from the ventricular surface. Scale bars, 50 μm (left panel) and 20

μm (insets).

See also Figure S4 and Table S2.
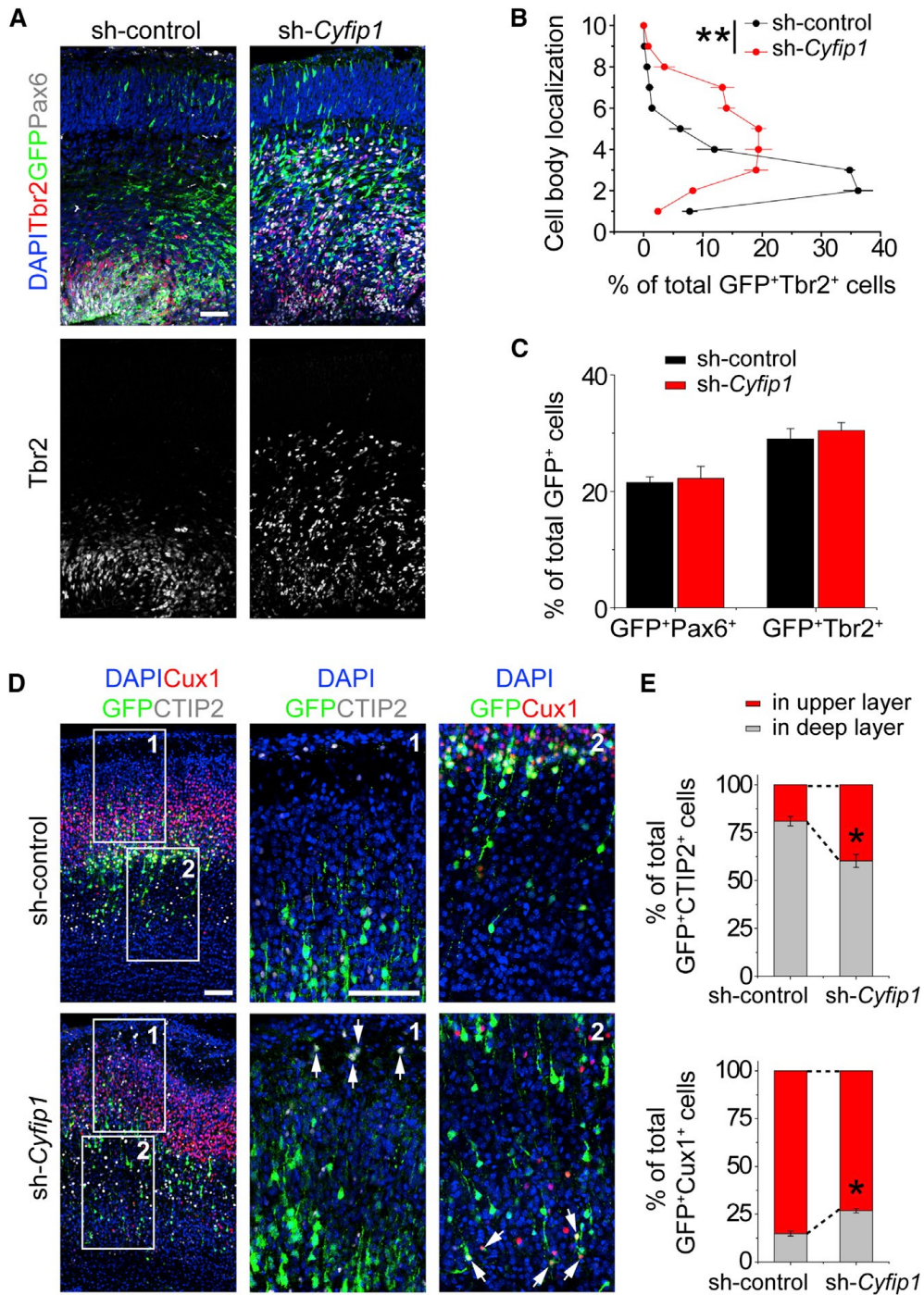
Figure 5. Ectopic placement of intermediate progenitor cells and cortical neurons upon CYFIP1 knockdown in RGCs

(A-C) Ectopic placement of intermediate progenitor cells (IPCs) upon CYFIP1 knockdown in RGCs. E13.5 embryos were electroporated to co-express GFP and sh-

Cyfip1 or sh-control and examined at E16.5. Shown in (A) are sample confocal images of immunostaining for GFP, Pax6, Tbr2 and DAPI. Scale bar, 50 μm. Shown in (B) are quantifications of the distribution of GFP$^+$Tbr2$^+$ cells in the neocortex. The graph represents GFP$^+$Tbr2$^+$ cells in each of ten equal-size vertical bins expressed as the percentage of total GFP$^+$Tbr2$^+$ cells. Values represent mean $\pm$ SEM (n = 4-5 animals; **$p < 0.01$; Student's t-test). Shown in (C) are quantifications of percentages of GFP$^+$ cells that were Pax6$^+$ or Trb2$^+$. Values represent mean $\pm$ SEM (n = 4 animals; $p > 0.1$; Student's t-test).

(D-E) Ectopic placement of cortical neurons upon CYFIP1 knockdown in RGCs. Same as in (A-C), except that electroporated brains were examined at P5. Shown in (D) are sample confocal images of immunostaining for GFP, Cux1, and CTIP2. Right panels represent two different insets in the left panels. Arrows point to GFP$^+$CTIP2$^+$ or GFP$^+$Cux1$^+$ cells. Scale bars, 100 μm. Shown in (E) are quantifications of percentages of GFP$^+$CTIP2$^+$ cells (top panel) or GFP$^+$Cux1$^+$ cells (bottom panel) that were distributed in upper or deeper layers, respectively. The boundary between upper and lower layers was established at the apical limit of Cux1$^+$ cells. Values represent mean $\pm$ SEM (n = 4 animals; *$p < 0.05$; Student's t-test).

See also Table S2.
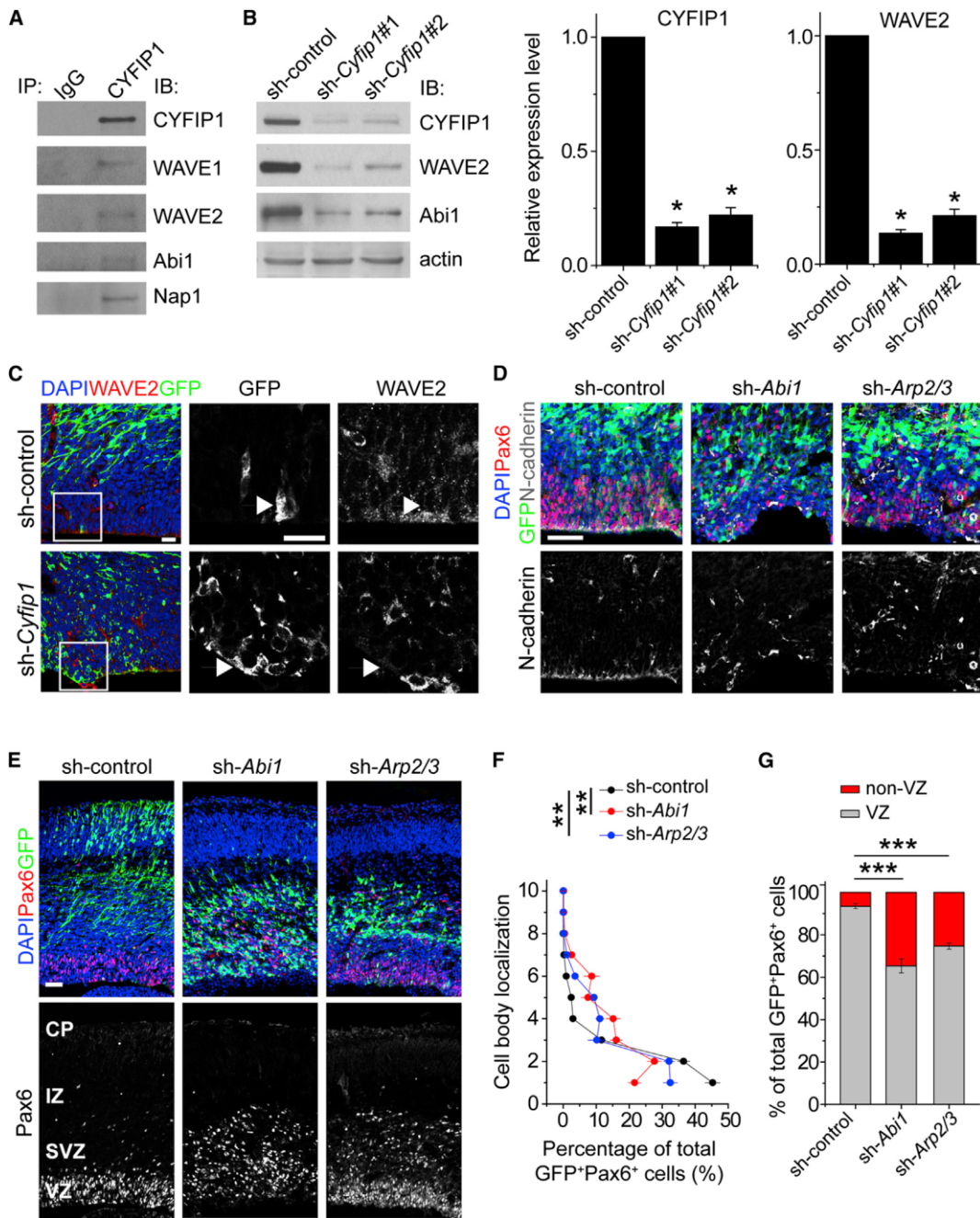
Figure 6. Critical role of CYFIP1 signalling in maintaining adherens junctions and proper placement of RGCs in the developing mouse cortex

(A) CYFIP1 is a component of WAVE complex in the developing mouse cortex. Shown are sample Western blot images of co-IP analysis using anti-CYFIP1 antibodies and E14.5 forebrain lysates.

(B) Reduced WAVE2 protein levels by CYFIP1 knockdown in mouse NPCs. Mouse NPCs were infected with retroviruses expressing sh-control, or sh-*Cyfip1* (#1 or #2) and then subjected to Western blot analyses 3 days later. Shown are sample Western blot images and quantifications of CYFIP1 and WAVE2 protein levels. Values represent mean $\pm$ SEM (n = 3; **p < 0.01; Student's t-test).

(C) Reduced WAVE2 protein levels at the ventricular surface in E16.5 neocortices in vivo. E13.5 embryos were electroporated to co-express GFP and sh-*Cyfip1* or sh-control and examined at E16.5. Shown are sample confocal images of immunostaining for GFP, WAVE2 and DAPI. Scale bar, 20 μm.

(D-G) Similar RGC defects among knockdown of CYFIP1, WAVE complex component Abi1, or downstream effectors Arp2/3. E13.5 embryos were electroporated to co-express GFP and sh-*Abi1* or sh-*Arp2*/sh-*Arp3* (double knockdown), and examined at E16.5. Shown in (D) are sample confocal images of immunostaining for GFP, Pax6, N-cadherin and DAPI. Shown in (E) are sample confocal images of immunostaining for GFP, Pax6, and DAPI. Scale bars, 50 μm. Also shown are two different quantifications of the distribution of GFP$^+$Pax6$^+$ cells in the neocortex among the different experiments, similar as in Figure 4B. Values represent mean $\pm$ SEM (n = 4 animals; **p < 0.01; ***p < 0.001; Student's t-test).

See also Figure S5 and Tables S2 and S3.

A

Effect	DF	Wald Chi-Square	p
American (LIBD/CBDB)	1	3.6722	0.0553
American (GRU)	1	2.0817	0.1491
German (MUN)	1	1.2778	0.2583
Scottish (ABE)	1	1.5369	0.2151
Combined sample:			
Additive model	1	8.5387	0.0035
Genotypic model	4	14.9641	0.0048

B

ACTR2*rs268864	*CYFIP1//NIPA1**rs4778334 Genotype	Reference	Estimate	SE	P	Adj P	OR	95% Confidence Limit Lower	Upper	p*
AA(=0)										0.0244
	CC(=0)	TT	-0.3343	0.1246	0.0073	0.0219	0.716	0.561	0.914	
	CT(=1)	TT	-0.2588	0.1270	0.0416	0.1248	0.772	0.602	0.990	
AG(=1)										0.4976
	CC(=0)	TT	0.1524	0.2080	0.4638	1	1.165	0.775	1.751	
	CT(=1)	TT	0.2359	0.2130	0.2680	0.8040	1.266	0.834	1.922	
GG(=2)										0.0103
	CC(=0)	TT	2.4106	1.0979	0.0281	0.0844	11.140	1.295	5.821	
	CT(=1)	TT	1.5172	1.1101	0.1717	0.5152	4.560	0.518	40.166	

Figure 7. Epistatic interaction of gene expression-associated variants of the WAVE signalling components for risk of schizophrenia

(A) Interaction analysis of SNPs rs2688674*ACTR2 and rs4778334*CYFIP1-NIPA1 in combined samples of four cohorts in European ancestry population. Analysis was performed adjusting for sex and cohort effect. DF, degree of freedom.

(B) Effect of interaction by genotypes on risk of schizophrenia from a logistic regression model based on genotypic interaction of *ACTR2* and *CYFIP1* in combined samples of four cohorts. Adj p is p value after adjusting for multiple testing from post-hoc analysis. SNPs were coded as 0, 1 and 2 for number of minor alleles.

See also Figure S6 and Tables S4, S5 and S6.

Chapter 3

Transcriptional dysregulation of synaptic genes in a human iPSC model of major mental disorders

Zhexing Wen[1,2]*, Ha Nam Nguyen[1,3]*, Ziyuan Guo[4]*, Matthew A. Lalli[5], Xinyuan Wang[1,6], Yijing Su[1,2], Nam-Shik Kim[1,2], Ki-Jun Yoon[1,2], Jaehoon Shin[1,3], Ce Zhang[1,2], Georgia Makri[1,2], David Nauen[1,7], Huimei Yu[1,2], Elmer Guzman[5], Cheng-Hsuan Chiang[1,2,8], Nadine Yoritomo[9], Kozo Kaibuchi[10], Jizhong Zou[1,11], Kimberly M. Christian[1,2], Linzhao Cheng[1,11], Christopher A. Ross[3,8,9], Russell L. Magolis[3,8,9#], Gong Chen[4#], Kenneth S. Kosik[5#], Hongjun Song[1,2,3,8#], and Guo-li Ming[1,2,3,8#]

[1]Institute for Cell Engineering, [2]Department of Neurology, [3]Graduate Program in Cellular and Molecular Medicine, [7]Department of Pathology, [8]The Solomon Snyder Department of Neuroscience, [9]Department of Psychiatry and Behavioral Sciences, [11]Department of Medicine, Johns Hopkins University School of Medicine, Baltimore, MD 21205, USA.

[4]Department of Biology, Huck Institutes of Life Sciences, The Pennsylvania State University, University Park, PA 16802, USA.

[5]Neuroscience Research Institute, Department of Molecular Cellular and Developmental Biology, Biomolecular Science and Engineering Program, University of California, Santa Barbara, CA 93106, USA.

[6]School of Basic Medical Sciences, Fudan University, Shanghai, PRC.

[10]Department of Cell Pharmacology, Nagoya University Graduate School of Medicine, Showa, Nagoya, Aichi, Japan.

*: These authors contributed equally to this work;

#: Co-senior authors.

Correspondence should be addressed to:

Hongjun Song, Ph.D. (E-mail: shongju1@jhmi.edu)

Guo-li Ming, M.D. & Ph.D. (E-mail: gming1@jhmi.edu)

Dysregulated neurodevelopment with altered structural and functional connectivity is believed to underlie many neuropsychiatric disorders[1] and "a disease of synapses" is the major hypothesis for the biological basis of schizophrenia[2]. While this hypothesis has gained indirect support from human post-mortem brain analyses[2-4] and genetic studies[5-10], little is known about the pathophysiology of synapses in patient neurons and how susceptibility genes for mental disorders could lead to synaptic deficits in humans. Genetics of most psychiatric disorders are extremely complex due to multiple susceptibility variants with low penetrance and variable phenotypes[11]. Rare, multiply affected, large families in which a single genetic locus is likely to be responsible for conferring susceptibility have proven invaluable for the study of complex disorders. Here we generated induced pluripotent stem cells (iPSCs) from four members of a family in which a frame-shift mutation of *Disrupted-in-schizophrenia-1* (*DISC1*) co-segregated with psychiatric disorders and we further produced different isogenic iPSC lines via gene editing. We showed that mutant DISC1 causes synaptic vesicle release deficits in iPSC-derived forebrain neurons. Mutant DISC1 depletes wild-type DISC1 and, furthermore, dysregulates expression of many genes related to synapses and psychiatric disorders in human forebrain neurons. Our study reveals that a psychiatric disorder-relevant mutation causes synapse deficits and transcriptional dysregulation and our findings provide novel insight into the molecular and synaptic etiopathology of psychiatric disorders.

  DISC1 was originally identified at the breakpoint of a balanced chromosomal translocation that co-segregated with schizophrenia, bipolar disorder and recurrent major

depression in a large Scottish family[12]. Another rare mutation of a 4 base-pair (bp) frame-shift deletion at the *DISC1* C-terminus was later discovered in a smaller American family (Pedigree H), which shares many similarities with the Scottish pedigree[13]. *DISC1* variants and polymorphisms have since been found to be associated with schizophrenia, bipolar disorder, major depression, and autism, and animal studies support a critical contribution of DISC1 to the etiopathology of major mental disorders[12], including regulating neuronal development and synapse formation[14]. Little is known about DISC1 function and dysfunction in human neurons.

Pluripotent stem cells reprogrammed from patient somatic cells offer a new way to investigate mechanisms underlying complex human diseases[15]. Using an episomal non-integrating approach[16] we establish iPSC lines from Pedigree H[13], including two patients with the frame-shift *DISC1* mutation (D2/schizophrenia and D3/major depression) and two unaffected members without the mutation (C2 and C3; Fig. 1a). We also included an unrelated healthy individual as an additional control (C1). We performed extensive quality control analyses and selected two iPSC lines from each individual for detailed studies (Extended Data Fig. 1 and Extended Data Table 1a).

We differentiated iPSCs into forebrain-specific human neural progenitor cells (hNPCs) expressing NESTIN, PAX6, EMX-1, FOXG1 and OTX2 (Fig. 1b; Extended data Fig. 2a-b and Extended Data Table 1b), and then into MAP2AB$^+$ neurons (99.92 $\pm$ 0.08%; n = 5). About 90% of neurons expressed VGLUT1 or α-CAMKII, indicative of glutamatergic neurons, while few neurons expressed VGAT or GAD67 (GABAergic), and even fewer expressed TH (dopaminergic; Fig. 1c and Extended Data Fig. 3). These neurons express different cortical layer markers, including TBR1, CTIP2, BRN2 and SATB2 (Fig. 1d). Quantitative analyses showed no differences in neuronal subtype differentiation among all lines (Fig. 1c-d and Extended Data Fig. 3).

The mutant *DISC1* allele is predicted to generate a frame-shift mutant DISC1 protein (mDISC1) with 9 *de novo* amino acids at the C-terminus[13] (Extended Data Fig. 4a). Quantitative real-time PCR (qPCR) analysis of a common exon 2 showed similar mRNA levels in different neurons (Extended Data Fig. 4b and Extended Data Table 1c). Strikingly, D2 and D3 neurons only expressed ~ 20% of the total DISC1 protein detected in control neurons using antibodies[17] that recognized both human full-length wild-type DISC1 (wDISC1) and mDISC1 when expressed in HEK293 cells (Fig. 1e). DISC1 interacts with itself and forms multimers, and sometimes aggregates[18]. Given that patients are heterozygous for the *DISC1* mutation (Extended Data Fig. 1f), this result suggested a model that mDISC1 interacts with wDISC1 to form aggregates and deplete soluble DISC1. Indeed, differentially tagged wDISC1 and mDISC1 co-immunoprecipitated when co-expressed in HEK293 cells (Extended Data Fig. 4c). mDISC1 significantly decreased soluble wDISC1 proteins in a dose-dependent manner and, furthermore, increased wDISC1 ubiquitination (Extended Data Fig. 4d-e). These results suggest a mechanism distinct from *DISC1* haploinsufficiency in mutant human neurons.

We next examined human forebrain neuron development. As in animal models[14], quantitative analyses showed both increased soma size and total dendritic length at 1 and 2 weeks after neuronal differentiation for mutant neurons; however, these properties became indistinguishable from control neurons at 3 and 4 weeks (Extended Data Fig. 5). Electrophysiological recordings of neurons did not show any consistent changes in their I-V relationship at 4 weeks after differentiation (Extended Data Fig. 6). To examine synapse formation, we immunostained synaptic vesicle protein SV2 (Fig. 2a), which is associated with mature synaptic vesicles and regulates presynaptic release[19,20]. The density of SV2+ synaptic boutons was significantly reduced in D2 and D3 neurons

compared to control neurons at both 4 and 6 weeks (Fig. 2b). We next performed whole-cell patch-clamp recordings of human neurons of similar densities co-cultured on astrocytes[21] (Fig. 2c). The frequency of excitatory spontaneous synaptic currents (SSCs), but not the amplitude, was significantly lower for D2-1 and D3-1 neurons compared to those of C3-1 neurons at both 4 and 6 weeks (Fig. 2d), suggesting a presynaptic defect in synaptic release. Results appeared to be more complex when neurons derived from outside of the pedigree (C1) were compared. D2-1 neurons exhibited markedly reduced SSC frequency and amplitude compared to C1-1 neurons at 4 weeks and slightly reduced frequency and amplitude at 6 weeks (Fig. 2d). For D3-1 neurons, similar results of reduced SSC frequency, but not amplitude, were observed when compared to C1-1 or C3-1 neurons at 4 or 6 weeks (Fig. 2d). While uniform results were obtained from comparison of neurons derived from the same family, all electrophysiological data showed functional synaptic transmission deficits in *DISC1* mutant neurons and further suggested a component of presynaptic dysfunction. Indeed, quantitative FM1-43 imaging analyses revealed a significant defect in depolarization-induced vesicle release for mutant neurons compared to control neurons (Fig. 2e).

To address whether the *DISC1* mutation is necessary and/or sufficient for observed synaptic defects, we generated different types of isogenic iPSC lines using transcription activator-like effector nuclease (TALEN; Fig. 3a). First, we corrected the 4-bp deletion in one mutant *DISC1* iPSC line (D3-2-6R). Second, we introduced the 4-bp deletion into two control iPSC lines, one within the pedigree (C3-1-3M) and, importantly, one outside of the pedigree (C1-2-5M) to control for potential effects of family genetic background. We confirmed successful gene editing by Sanger sequencing and validated the quality of targeted iPSCs (Extended Data Fig. 7). As expected, the total DISC1 protein was rescued in D3-2-6R neurons to a level comparable with control neurons, and

reduced in C1-2-5M and C3-1-3M neurons to a level similar to *DISC1* mutant neurons (Fig. 3b).

We next compared forebrain neurons derived from isogenic and parental iPSC lines in parallel. Deficits in the density of SV2$^+$ synaptic boutons were rescued in D3-2-6R neurons and recapitulated in C1-2-5M and C3-1-3M neurons (Fig. 3c). To examine morphological synapses further, we co-immunostained neurons with presynaptic marker SYNAPSIN1 (SYN1) and postsynaptic marker PSD95 (Fig. 3d). Quantification using the SYN1/PSD95 pair as a synapse marker showed reduced density in mDISC1-dependent fashion (Fig. 3d). Functional electrophysiological recording and FM-imaging analyses also confirmed mDISC1-dependent presynaptic release defects (Fig. 3e-f). These results, from three different isogenic iPSC lines, including the knock-in line from outside of the pedigree, established a causal role for the *DISC1* mutation in synaptic defects of human neurons and suggested a pathogenic nature of this *DISC1* mutation at the cellular level.

To gain molecular insight into how this pathogenic *DISC1* mutation causes synaptic defects, we performed RNA-seq analysis of 4 week-old forebrain neurons derived from a control (C3-1) and two mutant (D2-1 and D3-2) iPSC lines in triplicate (Extended Data Table 2a). There were a large number of differentially expressed genes between C3-1 and D2-1/D3-2 neurons (FDR < 5%; Fig. 4a and Extended Data Table 2b-c), while the expression profiles of D2-1 and D3-2 were very similar (Extended Data Fig. 8a). Results from qPCR analyses of selected genes using independent samples of C3-1 and D2-1 neurons were consistent with RNA-seq data (Extended Data Fig. 8b). Detailed bioinformatic analyses revealed several striking features of differentially expressed genes. First, top three significantly enriched categories from GO analysis were "synaptic transmission", "nervous system development" and "dendritic spine" (Fig. 4a and

Extended Data Table 2d). Second, a large number of genes encoding DISC1-interacting proteins[22] were differentially expressed (Fig. 4b). This result is surprising because previous studies have not appreciated the transcriptional relationship between DISC1 and its protein-interacting partners at a large scale. Third, 89 differentially expressed genes are linked to schizophrenia, bipolar disorder, depression and mental disorders (Fig. 4c and Extended Data Table 2e). Thus, mDISC1 also functions as a hub for transcriptional regulation of genes implicated in psychiatric disorders.

To extend these results and establish a causal link between differential gene expression and the *DISC1* mutation, we performed qPCR analyses of synapse-related genes using forebrain neurons derived from multiple isogenic iPSC lines. Differential expression of many genes was found to be mDISC1-dependent (Fig. 4d and Extended Data Fig. 8c). Consistent with a presynaptic defect, mRNAs for a number of presynaptic proteins, including SYN isoforms 2 and 3, SYNAPTOPHYSIN (SYP), SYNAPTOPORIN (SYNPR), NRNX1, and VAMP2, were increased in neurons carrying the *DISC1* mutation (Fig. 4d and Extended Data Fig. 8c). Western blot analyses further confirmed increased protein expression of SYN and SYP in mutant neurons (Fig. 4e and Extended Data Fig. 8d). Previous studies in multiple neuronal systems have shown that elevated synapsin levels suppress pre-synaptic neurotransmitter release[23,24]. In contrast, some postsynaptically localized proteins, including GLUR1 and NR1, were not affected at either mRNA or protein level in bulk preparations (Fig. 4d-e and Extended Data Fig. 8c-d). We also observed differential expression of several transporters (Fig. 4d). Notably, the transcription factor MEF2C was drastically increased at mRNA and protein levels in mutant neurons (Fig. 4d-e and Extended Data Fig. 8c-d). In mice, MEF2C functions to restrict glutamatergic synapse numbers[25] and elevated MEF2C leads to decreased

frequency, but not amplitude of SSCs[26], which resembles what we observed in *DISC1* mutant human neurons and suggests an underlying molecular mechanism.

Our study of human forebrain neurons derived from a collection of patient iPSCs and different isogenic lines suggests a model that susceptibility genes for major psychiatric disorders could affect synaptic function via large-scale transcriptional dysregulation in human neurons. Our results illustrate a potential mechanistic link in human patient neurons for three major hypotheses of complex psychiatric disorders – genetic risk, aberrant neurodevelopment, and synaptic dysfunction. We have developed an enhanced iPSC model for schizophrenia and major mental disorders at the cellular level[27] that includes a high-penetrance and disease-related genotype, iPSC lines from multiple members of the same family, different types of isogenic lines to address causality, and a relatively homogeneous neuronal subtype population. A key challenge and opportunity for iPSC disease-modeling is to generate new insight into pathophysiology, as opposed to confirming existing hypotheses or validating previous results from animal models. Much of our knowledge of DISC1 functions has come from understanding the biology of DISC1-interacting proteins and the function of these protein complexes, derived mostly from rodent models based on overexpression of truncated DISC1 proteins or loss-of-function via genetic deletion or shRNA knockdown[12]. Unexpectedly, we found that disease-relevant, endogenous mutant DISC1 in human neurons causes large-scale transcriptional dysregulation of genes related to synapses, DISC1-interacting proteins, and psychiatric disorders. Our DISC1 mutant phenotypes partially overlap with those observed in previous studies of neurons derived from idiopathic schizophrenia patient iPSCs[28-30], including decreased synaptic connectivity and transcriptional dysregulation of shared genes, suggesting the potential of a common disease mechanism. Our collection of iPSC lines and identified cellular phenotypes also

provide a platform both for mechanism-guided exploration of therapeutic compounds in correcting synaptic defects of human neurons and for nonbiased large-scale screens.

Methods Summary

iPSC lines were derived from skin fibroblasts using a non-integrating approach and subject to full characterization similarly as previously described[16]. Isogenic iPSC lines were generated using the TALEN strategy. iPSC lines were differentiated into forebrain-specific hNPCs and further to cortical neurons for characterization using immunocytochemistry, electrophysiology, FM1-43 imaging, Western blot and gene expression analyses. See the full Methods section for detailed description.

Reference

1 Weinberger, D. R. Implications of normal brain development for the pathogenesis of schizophrenia. *Arch Gen Psychiatry* **44**, 660-669 (1987).

2 Mirnics, K., Middleton, F. A., Lewis, D. A. & Levitt, P. Analysis of complex brain disorders with gene expression microarrays: schizophrenia as a disease of the synapse. *Trends Neurosci* **24**, 479-486 (2001).

3 Johnson, R. D., Oliver, P. L. & Davies, K. E. SNARE proteins and schizophrenia: linking synaptic and neurodevelopmental hypotheses. *Acta Biochim Pol* **55**, 619-628 (2008).

4 Honer, W. G. & Young, C. E. Presynaptic proteins and schizophrenia. *Int Rev Neurobiol* **59**, 175-199 (2004).

5 Gulsuner, S. *et al.* Spatial and temporal mapping of de novo mutations in schizophrenia to a fetal prefrontal cortical network. *Cell* **154**, 518-529 (2013).

6   Kenny, E. M. *et al.* Excess of rare novel loss-of-function variants in synaptic genes in schizophrenia and autism spectrum disorders. *Mol Psychiatry* (2013).

7   Malhotra, D. *et al.* High frequencies of de novo CNVs in bipolar disorder and schizophrenia. *Neuron* **72**, 951-963 (2011).

8   Purcell, S. M. *et al.* A polygenic burden of rare disruptive mutations in schizophrenia. *Nature* (2014).

9   Fromer, M. *et al.* De novo mutations in schizophrenia implicate synaptic networks. *Nature* (2014).

10   Lips, E. S. *et al.* Functional gene group analysis identifies synaptic gene groups as risk factor for schizophrenia. *Mol Psychiatry* **17**, 996-1006 (2012).

11   Sullivan, P. F., Daly, M. J. & O'Donovan, M. Genetic architectures of psychiatric disorders: the emerging picture and its implications. *Nat Rev Genet* **13**, 537-551 (2012).

12   Thomson, P. A. *et al.* DISC1 genetics, biology and psychiatric illness. *Front Biol (Beijing)* **8**, 1-31 (2013).

13   Sachs, N. A. *et al.* A frameshift mutation in Disrupted in Schizophrenia 1 in an American family with schizophrenia and schizoaffective disorder. *Mol Psychiatry* **10**, 758-764 (2005).

14   Duan, X. *et al.* Disrupted-In-Schizophrenia 1 regulates integration of newly generated neurons in the adult brain. *Cell* **130**, 1146-1158 (2007).

15   Christian, K., Song, H. & Ming, G. Application of reprogrammed patient cells to investigate the etiology of neurological and psychiatric disorders. *Frontiers in Biology* **7**, 179-188 (2012).

16   Chiang, C. H. *et al.* Integration-free induced pluripotent stem cells derived from schizophrenia patients with a DISC1 mutation. *Mol Psychiatry* **16**, 358-360 (2011).

17   Kuroda, K. *et al.* Behavioral alterations associated with targeted disruption of exons 2 and 3 of the Disc1 gene in the mouse. *Hum Mol Genet* **20**, 4666-4683 (2011).

18   Leliveld, S. R. *et al.* Insolubility of disrupted-in-schizophrenia 1 disrupts oligomer-dependent interactions with nuclear distribution element 1 and is associated with sporadic mental disease. *J Neurosci* **28**, 3839-3845 (2008).

19   Custer, K. L., Austin, N. S., Sullivan, J. M. & Bajjalieh, S. M. Synaptic vesicle protein 2 enhances release probability at quiescent synapses. *J Neurosci* **26**, 1303-1313 (2006).

20   Chang, W. P. & Sudhof, T. C. SV2 renders primed synaptic vesicles competent for Ca2+ -induced exocytosis. *J Neurosci* **29**, 883-897 (2009).

21   Marchetto, M. C. *et al.* A model for neural development and treatment of Rett syndrome using human induced pluripotent stem cells. *Cell* **143**, 527-539 (2010).

22   Camargo, L. M. *et al.* Disrupted in Schizophrenia 1 Interactome: evidence for the close connectivity of risk genes and a potential synaptic basis for schizophrenia. *Mol Psychiatry* **12**, 74-86 (2007).

23   Hackett, J. T., Cochran, S. L., Greenfield, L. J., Jr., Brosius, D. C. & Ueda, T. Synapsin I injected presynaptically into goldfish mauthner axons reduces quantal synaptic transmission. *J Neurophysiol* **63**, 701-706 (1990).

24   Rosahl, T. W. *et al.* Short-term synaptic plasticity is altered in mice lacking synapsin I. *Cell* **75**, 661-670 (1993).

25   Flavell, S. W. *et al.* Activity-dependent regulation of MEF2 transcription factors suppresses excitatory synapse number. *Science* **311**, 1008-1012 (2006).

26   Barbosa, A. C. *et al.* MEF2C, a transcription factor that facilitates learning and memory by negative regulation of synapse numbers and function. *Proc Natl Acad Sci U S A* **105**, 9391-9396 (2008).

27   Wright, R., Rethelyi, J. M. & Gage, F. H. Enhancing Induced Pluripotent Stem Cell Models of Schizophrenia. *JAMA Psychiatry* (2013).

28   Brennand, K. J. *et al.* Modelling schizophrenia using human induced pluripotent stem cells. *Nature* **473**, 221-225 (2011).

29   Yu, D. X. *et al.* Modeling hippocampal neurogenesis using human pluripotent stem cells. *Stem Cell Reports* **2**, 295-310 (2014).

30   Brennand, K. *et al.* Phenotypic differences in hiPSC NPCs derived from patients with schizophrenia. *Mol Psychiatry* (2014).

31   Ma, D. K. *et al.* Neuronal activity-induced Gadd45b promotes epigenetic DNA demethylation and adult neurogenesis. *Science* **323**, 1074-1077 (2009).

32   Cermak, T. *et al.* Efficient design and assembly of custom TALEN and other TAL effector-based constructs for DNA targeting. *Nucleic Acids Res* **39**, e82 (2011).

33   Song, H. J., Stevens, C. F. & Gage, F. H. Neural stem cells from adult hippocampus develop essential properties of functional CNS neurons. *Nat Neurosci* **5**, 438-445 (2002).

34   Ho, S. Y. *et al.* NeurphologyJ: an automatic neuronal morphology quantification method and its application in pharmacological discovery. *BMC Bioinformatics* **12**, 230 (2011).

35   Trapnell, C. *et al.* Transcript assembly and quantification by RNA-Seq reveals unannotated transcripts and isoform switching during cell differentiation. *Nat Biotechnol* **28**, 511-515 (2010).

36   Langmead, B. & Salzberg, S. L. Fast gapped-read alignment with Bowtie 2. *Nat Methods* **9**, 357-359 (2012).

37   Wang, L., Wang, S. & Li, W. RSeQC: quality control of RNA-seq experiments. *Bioinformatics* **28**, 2184-2185 (2012).

38   Robinson, M. D., McCarthy, D. J. & Smyth, G. K. edgeR: a Bioconductor package for differential expression analysis of digital gene expression data. *Bioinformatics* **26**, 139-140 (2010).

39   Wang, J., Duncan, D., Shi, Z. & Zhang, B. WEB-based GEne SeT AnaLysis Toolkit (WebGestalt): update 2013. *Nucleic Acids Res* **41**, W77-83 (2013).

Author Contributions: Z.W. led and was involved in every aspect of the project. H.N.N generated isogenic iPSC lines. Z.G and G.C. performed electrophysiology analyses. M.A.L., E.G. and K.S.K. performed RNA-seq analyses. X.W., Y.S., N-S.K., J-j.Y., J.S.,

C.Z.,G.M., D.N., H.Y., C-H. C. and K.M.C. helped data collection. N.Y., C.A.R. and R.L.M. obtained original skin biopsies from 4 patients. J.Z. and L.C. helped with TALEN design. G-l.M., H.S. and Z.W. designed the project and wrote the manuscript.

Methods

Generation and characterization of patient iPSCs and isogenic iPSC lines. Skin biopsy samples were obtained from four individuals in a previously characterized American family, Pedigree H[13] (Fig. 1a). C1 fibroblasts were from ATCC (CRL-2097). All studies followed institutional IRB, ISCRO and animal protocols approved by Johns Hopkins University School of Medicine. Informed consents were obtained from individuals from Pedigree H. Mouse embryonic fibroblasts (MEFs) were derived from E13.5 CF-1 mouse embryos[16]. Fibroblasts were cultured in Dulbecco's modified Eagle's medium (DMEM, Mediatech Inc.) supplemented with 10% fetal bovine serum (FBS, HyClone) and 2 mM L-glutamine (Invitrogen).

iPSCs were generated with the EBV-based vectors as previously described[16]. Briefly, plasmids pEP4 EO2S ET2K (Addgene Plasmid 20927), pEP4 EO2S EN2L (Addgene Plasmid 20922), and pEP4 EO2S EM2K (Addgene Plasmid 20923) were transfected into human fibroblasts by Amaxa Nucleofector (Lonza; program U-023) at a concentration of 2 μg per 100 μl electroporation solution per 2×10^6 cells. Colonies of iPSCs were manually picked after 3-6 weeks for further expansion and characterization. Lack of vector integration was confirmed by qPCR analysis as previously described[16].

Two lines from each individual that passed stringent criteria were used for the current study (Extended Data Table 1a). iPSCs (passage ≤ 35) were cultured on irradiated MEFs in human iPSC medium consisting of D-MEM/F12 (Invitrogen), 20% Knockout Serum Replacement (KSR, Invitrogen), 2 mM L-glutamine (Invitrogen), 100 μM MEM NEAA (Invitrogen), 100 μM β-mercaptoethanol (Invitrogen), and 10 ng/ml human basic FGF (bFGF, PeproTech) as described[16]. For feeder-free culture of iPSCs, cells were cultured on Matrigel (BD Biosciences) with mTeSR1 media (Stem Cell Technologies). Media were changed daily and iPSC lines were passaged by collagenase (Invitrogen, 1 mg/ml in D-MEM/F12 for 30 min at 37ºC).

Karyotyping analysis by standard G-banding technique was carried out by the Cytogenetics Core Facility at the Johns Hopkins Hospital or Cell Line Genetics Inc. Results were interpreted by clinical laboratory specialists of the Cytogenetics Core or Cell Line Genetics. Genotyping analysis was performed as described previously[16]. Genomic DNA of fibroblasts and derived iPSCs was extracted by DNeasy Blood & Tissue Kit (Qiagen) following the manufacturer's recommended protocol. A pair of specific primers was used to amplify the region around the 4-bp deletion (Extended Data Table 1c). PCR products were cloned by TA cloning and sequenced. Bisulfite genomic sequencing was carried out with the EZ DNA Methylation-Direct Kit (Zymo Research) as previously described[31]. After bisulfite conversion of genomic DNA from iPSCs, primers specific to human OCT4 and NANOG promoters (Expended Data Table 1c) were used to amplify genomic DNA sequences with Platinum Taq DNA Polymerase High Fidelity (Invitrogen) for sequencing.

To assess the *in vivo* pluripotency of iPSC lines, teratoma formation assays were performed[16]. iPSCs were injected subcutaneously into the dorsal flank of SCID mice. Animals were monitored and teratomas were dissected at 8 to 10 weeks post-injection.

Tissues were fixed in 10% neutralized formalin solution (Sigma). Embedding, sectioning and H&E staining were carried out by the Pathology Core Facility at the Johns Hopkins University Hospital.

TALEN designs and constructions were based on a Golden Gate Assembly protocol with modifications to the vector backbone[32]. Donor DNA vectors with a loxP-flanked PGK-Hygromycin cassette were cloned between 5' and 3' homology arms (Fig. 3a), which were amplified from genomic DNA of a healthy subject and a patient with the *DISC1* 4-bp mutation. For targeting, TALENs (4 μg DNA of each plasmid) and linearized donor vectors (10 μg DNA) were electroporated into individual iPSCs (1-2 x 10^6 cells pretreated with 5 μM ROCK inhibitor, Y-27632, Cellagentech) using Nucleofector 2b (Lonza; program A-023). Transfected cells were transferred onto a 6-well dish pre-plated with inactivated MEFs and supplemented with Y-27632 in standard iPSC medium. Positive colonies were selected by 10 μg/ml Hygromycin B (Invitrogen) after 5 days of culture or until small colonies appeared. Resistant colonies were sub-cloned and expanded in 48-well plates. Over 200 clonal lines were screened. The loxP-flanked PGK-Hygromycin cassette was removed by electroporation of a Cre Recombinase expression vector (4 μg DNA). Specific integration, correct genetic editing and efficient removal of PGK-Hygromycin cassette at each stage were verified by Sanger sequencing.

Differentiation of iPSCs into forebrain-specific neural progenitors and cortical neurons. The protocol is illustrated in Extended Data Fig. 2a. Specifically, iPSCs colonies were detached from the feeder layer with 1 mg/ml collagenase treatment for 1 hr and suspended in EB medium, consisting of FGF-2-free iPSC medium supplemented with 2 µM Dorsomorphin and 2 µM A-83, in non-treated polystyrene plates for 4 days

with a daily medium change. After 4 days, EB medium was replaced by neural induction medium (hNPC medium) consisting of DMEM/F12, N2 supplement, NEAA, 2 μg/ml heparin and 2 μM cyclopamine. The floating EBs were then transferred to matrigel-coated 6-well plates at day 7 to form neural tube-like rosettes. The attached rosettes were kept for 15 days with hNPC medium change every other day. On day 22, the rosettes were picked mechanically and transferred to low attachment plates (Corning) in hNPC medium containing B27. For neuronal differentiation, resuspended neural progenitor spheres were dissociated with Accutase at 37ºC for 10 min and placed onto Poly-D-Lysine/laminin-coated coverslips in the neuronal culture medium, consisting of Neurobasal medium supplemented with 2 mM L-glutamine, B27, 10 ng/ml BDNF and 10 ng/ml GDNF. Half of the medium was replaced once a week during continuous culturing. Neural progenitors were plated on a confluent layer of rodent astrocytes only for electrophysiological recordings as previously described[21,33]. These cultures exhibited similar neuronal densities and parallel cultures were used for recordings of different iPSC lines in a blind fashion.

Immunocytochemistry. Cells were fixed with 4% paraformaldehyde (Sigma) for 15 min at room temperature. Samples were permeabilized and blocked with 0.25% Triton X-100 (Sigma) and 10% donkey serum in PBS for 20 min as previously described[16]. Samples were then incubated with primary antibodies (Extended Data Table 1b) at 4ºC overnight, followed by incubation with secondary antibodies for 1 hr at room temperature. Antibodies were prepared in PBS containing 0.25% Triton X-100 and 10% donkey serum. Images were taken by Zeiss LSM 710 confocal microscope, or Zeiss Axiovert 200M microscope, and analyzed with ImageJ (NIH). Images were acquired with identical settings for parallel cultures. For analysis of synaptic bouton density, total SV2^{+} puncta

in a given image were counted by ImageJ Analyze Particles, and the total dendritic length were measured by ImageJ plugin NeurphologyJ[34]. The numbers of SYN1/PSD95 pairs were manually counted. The synaptic density was determined by D (D = total $SV2^+$ puncta or SYN1/PSD95 pair per 100 μm total dendritic length).

Electrophysiological and FM1-43 imaging analyses: Whole-cell patch-clamp recordings were performed using Multiclamp 700A patch-clamp amplifier (Molecular Devices, Palo Alto, CA) as previously described[21]. Briefly, the recording chamber was constantly perfused with a bath solution consisting of 128 mM NaCl, 30 mM glucose, 25 mM HEPES, 5 mM KCl, 2 mM $CaCl_2$, and 1 mM $MgCl_2$ (pH 7.3; 315-325 mOsm/L). Patch pipettes were pulled from borosilicate glass (3 - 5 MΩ) and filled with an internal solution consisting of 135 mM KGluconate, 10 mM Tris-phosphocreatine, 10 mM HEPES, 5 mM EGTA, 4 mM MgATP, and 0.5 mM Na_2GTP (pH 7.3). The series resistance was typically 10-30 MΩ. For SSC recording, the membrane potential was typically held at -70 mV. Drugs were applied through a gravity-driven drug delivery system (VC-6, Warner Hamden, CT). Data were acquired using pClamp 9 software (Molecular Devices, Palo Alto, CA), sampled at 10 kHz and filtered at 1 kHz. Spontaneous synaptic events were analyzed using MiniAnalysis software (Synaptosoft, Decatur, GA). All experiments were conducted at room temperature.

For monitoring synaptic vesicle release, human iPSC-derived neurons were loaded with 10 μM FM1-43 for 2 min in FM image buffer (FMIB, consisting of 170 mM NaCl, 3.5 mM KCl, 0.4 mM KH2PO4, 5 mM $NaHCO_3$, 1.2 mM Na_2SO_4, 1.2 mM $MgCl_2$, 1.3 mM $CaCl_2$, 5 mM glucose, 20 mM N-tris(hydroxymethyl)-methyl-2-aminoethane-sulfonic acid, pH 7.4, ~360 mOsmol) supplemented with 60 mM KCl, followed by wash with 10 μM FM1-43 in FMIB for 2 min. Subsequent washing was with FMIB for 5 min

followed by FMIB supplemented with 1 mM ADVASEP-7. FM1-43 imaging was performed on a Nikon TE2000 imaging system with a 20x objective. Neurons were perfused with FMIB for 1 min as the baseline, followed by stimulation with 60 mM KCl for 4 min. Cells were excited at FITC spectra, and the green fluorescence was collected as FM1-43 signal. Images were acquired every 5 sec and analyzed using NIH ImageJ software. The FM1-43 signal was determined by F ($F = (F_1-B_1)/(F_0-B_0)$), which was normalized to the mean fluorescence intensity measured at the baseline condition (set as 1).

qPCR and RNA-seq analyses: Human forebrain neurons without astrocyte co-culture were used for gene expression analyses. Total RNA was isolated using mirVana kit (Invitrogen) according to manufacturer's instructions. For qPCR, a total of 1 µg RNA was used to synthesize cDNA with the SuperScript® III First-Strand Synthesis System (Invitrogen). Quantitative RT-PCR was then performed using SYBR green (Applied Biosystems) and the StepOnePlus™ Real-Time PCR System (Applied Biosystems). Quantitative levels for all genes were normalized to the housekeeping gene GAPDH and expressed relative to the relevant control samples. All primer sequences are listed in Expended Data Table 3.

For deep RNA sequencing, libraries for three biological replicates of 4 week-old forebrain neurons derived from iPSCs of three individuals within the pedigree H (C3-1, D2-1 and D3-2) without astrocyte co-culture were prepared and sequenced on an Ion Proton Torrent. Libraries were prepared using the Ion Total RNA-Seq Kit v2 for Whole Transcriptome sequencing following the protocol provided by the manufacturer (Life Technologies, Carlsbad, CA). Briefly, poly(A)-enriched mRNA samples were fragmented, Ion Adaptors were hybridized, and cDNA generated through reverse

transcription. Barcodes were added and the libraries were amplified for sequencing. From the poly(A)+ RNA-Seq libraries, a total of 123 million reads were generated comprising between 9 and 34 million reads from each of the 9 samples (Extended Data Table 2a). Sequencing generated strand-specific single-end reads of variable length between 8-240 bp. Reads were mapped to the UCSC Human Reference Genome (hg19) using TopHat[35] (v2.0.10) and Bowtie[36] (v2.1.0). Resulting sequence alignment files were analyzed using RSeQC package for quality control[37]. Reads covering gene coding regions were counted with BEDTools and count data were analyzed for differential expression using edgeR[38] (v2.15.0). For Gene Ontology analysis, gene lists were obtained for disease enrichment from PharmGKB, KEGG pathways from the Encyclopedia of Genes and Genomes and gene ontology (GO) from AmiGO. IDs for each gene list are provided in Extended Data Table . P-values were calculated from a cumulative hypergeometric distribution, calculated at http://www.geneprof.org/GeneProf/tools/hypergeometric.jsp. The total population size was set to 20687. Additional gene ontology analysis was performed with WebGestalt[39].

DNA constructs and biochemical analyses: Full-length human DISC1 cDNA were amplified by PCR and subcloned with HA-tag through AgeI and EcoRV into the pFUGW vector. The 4-bp deletion mutation was introduced through synthesized long length PCR primer and cloned with flag-tag through AgeI and EcoRV into the pFUGW vector. All expression plasmids were confirmed by DNA sequencing.

HEK293 cells were cultured in Dulbecco's modified Eagle's medium (Invitrogen), supplemented with 10% FBS (GIBCO). Once reaching 70% confluence, the cells were transiently transfected with cDNA constructs using Lipofectamine 2000 (Invitrogen). Cells were harvested 48 hr after transfection for biochemical analyses. Cells were lysed

in RIPA buffer (150 mM NaCl, 1% Triton X-100, 0.5% sodium deoxycholate, 0.1% SDS; 50 mM Tris, pH 8.0) containing Complete Protease Inhibitor Cocktail (Roche). Samples were left on ice for 30 min and sonicated briefly. The insoluble fraction was removed by centrifugation at 15,000 rpm for 15 min at 4°C. Protein concentration was determined by BCA protein assay kit (Bio-Rad). 2X SDS sample buffer (Bio-Rad) containing 5% β-mercaptoethanol (Sigma) was added to equal amounts of protein. Proteins were then separated by 4-15% SDS PAGE (Bio-Rad) and transferred to nitrocellulose membrane (0.45 μm). 5% dried milk in TBST (Tris buffered saline with 0.1% Tween 20) was incubated for blocking, and membranes were applied with specific antibodies as listed in Extended Data Table 1b. After washing with TBST and incubation with horseradish peroxidase-conjugated anti-rabbit or anti-mouse IgG (Santa Cruz Biotechnology), the antigen-antibody was detected by chemiluminescence (ECL; Pierce) and X-ray film (GE Healthcare).

For immunoprecipitation experiments, cells were lysed using an IP lysis buffer containing 25 mM HEPES, pH 7.4, 1 mM EDTA, 10 mM NaCl, 0.5% Triton X-100, protease inhibitors cocktail (Roche) and 1 mM PMSF, except for the ubiquitination assay in which the IP lysis buffer contains 0.2% SDS (Extended Data Fig. 4e). Equal amount of protein was incubated overnight with Fast Flow Protein G agarose beads (Millipore) and mouse IgG or specific antibody in IP lysis buffer. After pull-down, protein-G beads were washed five times with IP washing buffer (25 mM HEPES, pH 7.4, 1 mM EDTA, 100 mM NaCl, 0.5% Triton X-100 and protease inhibitors cocktail (Roche) and boiled with 2X SDS sample buffer (Bio-Rad) containing 5% β-mercaptoethanol (Sigma). Western Blotting was then carried out with primary antibodies listed in Extended Data Table 1b.

Data collection and statistics

All experiments were replicated at least three times using iPSC lines indicated in Extended Data Table 1 and data from parallel cultures were acquired. The sample size and description of the sample collection are reported in each figure legend. Qualifications of synaptic puncta density, FM-imaging and electrophysiological analyses were performed in a blind fashion. Statistical analyses used for comparison are reported in each figure legends.

Figures and Legends

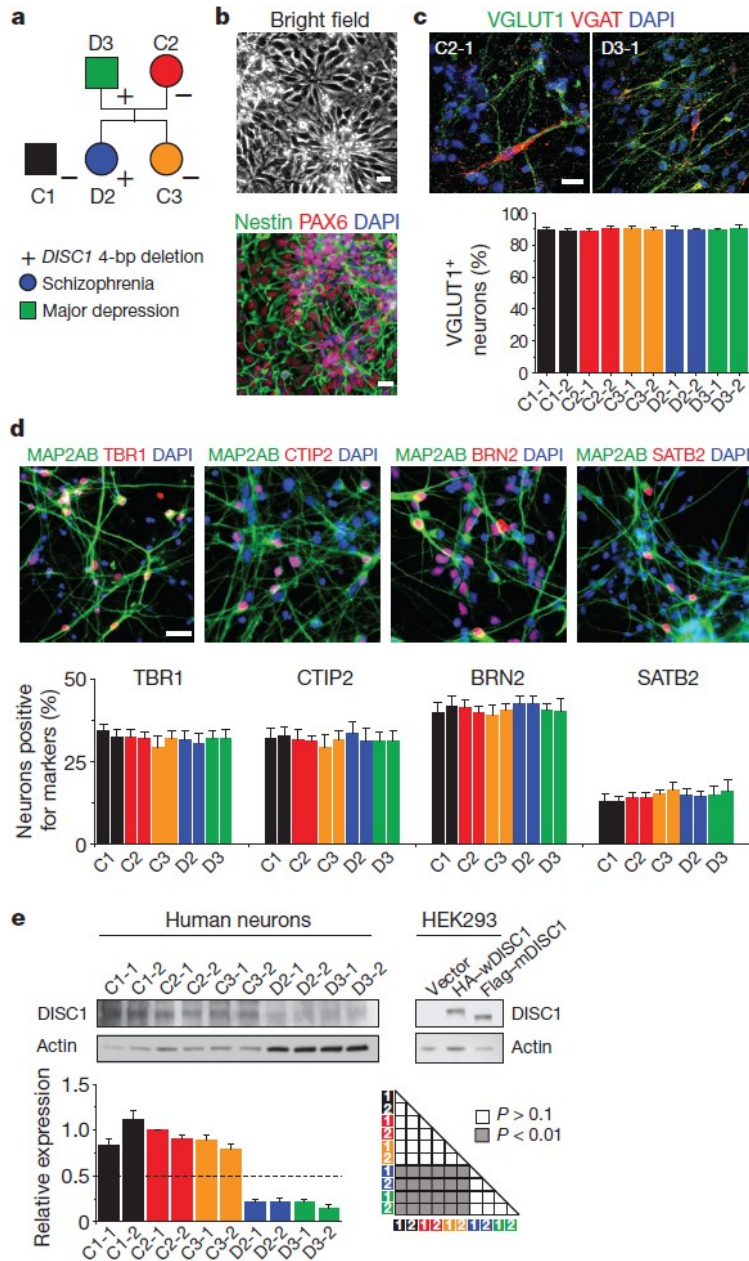**Figure 1. Normal neural differentiation, but markedly reduced total DISC1 protein levels in forebrain neurons derived from patient iPSCs carrying the *DISC1* mutation. a,** A schematic diagram of the pedigree for iPSC generation. In addition, iPSCs from a control individual outside of the pedigree (C1, male) were used in the current study. "+": one copy of the 4-bp deletion in the *DISC1* gene; "-": lack of the 4-bp

deletion in the *DISC1* gene. **b-d,** Neural differentiation of iPSCs. Shown in (**b**) are

sample bright field and confocal images of NESTIN and PAX6 immunostaining of

hNPCs. See Extended Data Fig. 2 for characterization of additional forebrain neural

progenitor markers. Shown in (**c**) are sample confocal images of immunostaining of

human neurons at 4 weeks after neuronal differentiation for VGLUT1 and VGAT, and

quantification of VGLUT1$^+$ neurons among different iPSC lines. Values represent mean

$\pm$ s.e.m. (n = 5 cultures). See Extended Data Fig. 3 for characterization of other markers.

Shown in (**d**) are sample confocal images of immunostaining for MAP2AB and neuronal

subtype markers of different cortical layers and quantification of neuronal subtype

differentiation among different iPSC lines. Values represent mean $\pm$ s.e.m. (n = 4

cultures). Scale bars: 20 μm. **e,** DISC1 protein levels in forebrain neurons derived from

different iPSC lines. Shown are sample Western blot images and quantification. Data

were normalized to that of ACTIN for sample loading and then normalized to C2-1 in the

same blot for comparison. Values represent mean $\pm$ s.e.m. (n = 3; ANOVA). Note that

the DISC1 antibodies used recognized both full-length human wDISC1 (HA-tagged) and

mDISC1 (Flag-tagged) exogenously expressed in HEK293 cells. More protein samples

from mutant neurons were loaded to show the presence but reduced levels of DISC1

protein in the sample image. See Fig. 3b for sample images with similar sample loading.
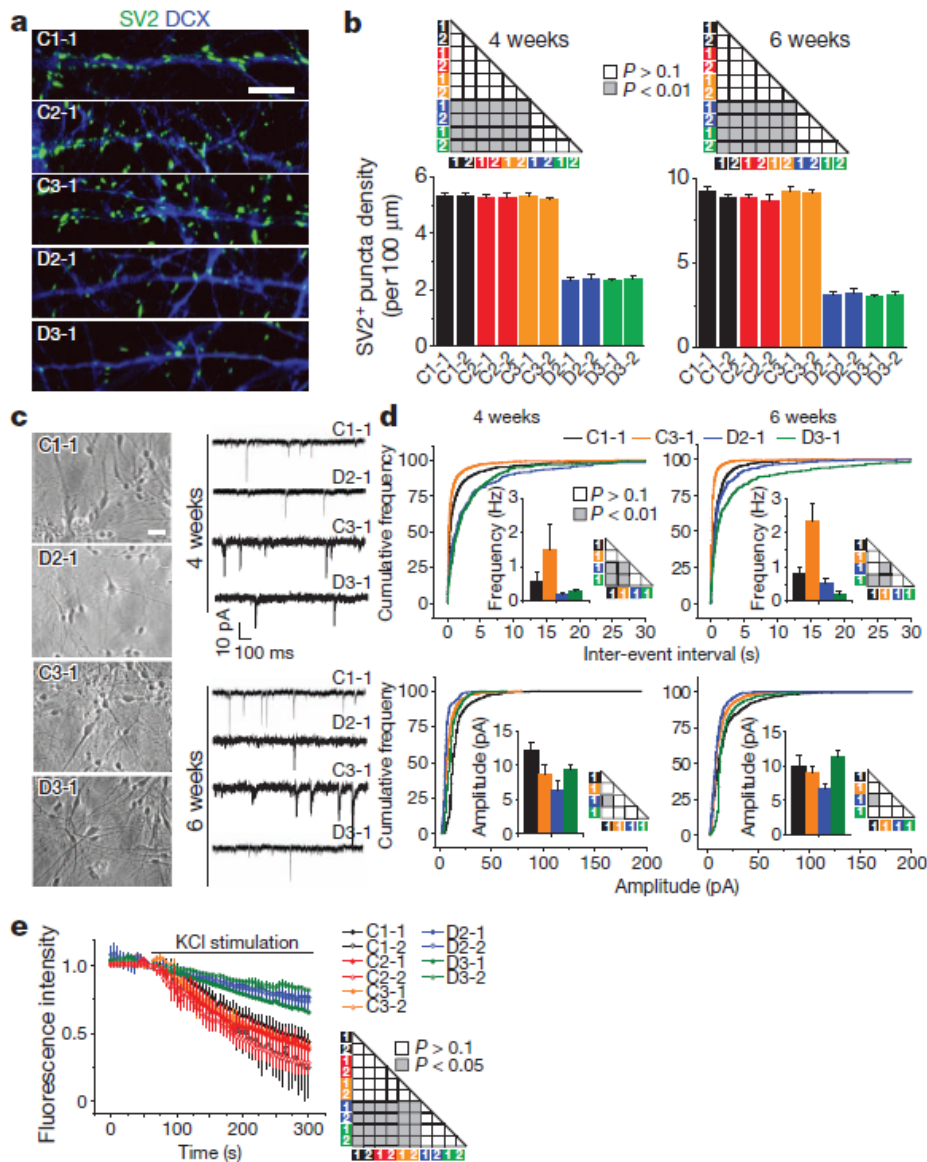
Figure 2. Defects of glutamatergic synapses in forebrain neurons carrying the

***DISC1* mutation. a-b,** Decreased density of SV2^{+} puncta by human forebrain neurons

derived from patient iPSC lines carrying the *DISC1* mutation compared to control lines.

Shown in (**a**) are sample confocal images of SV2 and DCX immunostaining of neurons

at 4 weeks. Scale bar: 20 μm. Shown in (**b**) are summaries of quantification of SV2^{+}

puncta density for neurons derived from two iPSC lines for each individual. Values

represent mean $\pm$ s.e.m. (n = 5 cultures; ANOVA). **c-d,** Defects in glutamatergic synaptic

transmission by *DISC1* mutant neurons. Forebrain hNPCs were co-cultured on confluent

astrocyte feeder layers. Shown in (**c**) are sample phase images of co-culture (Scale bar:

20 μm) and sample whole-cell voltage-clamp recording traces of excitatory spontaneous

synaptic currents (SSCs). Shown in (**d**) are distribution plots of SSC event intervals and

amplitudes (n = 10-12 neurons for each condition; Kolmogorov–Smirnov test). Mean

frequencies and amplitudes are also shown. **e,** Decreased vesicle release by *DISC1*

mutant neurons. Six week-old neurons were imaged for KCl (60 mM)-induced release of

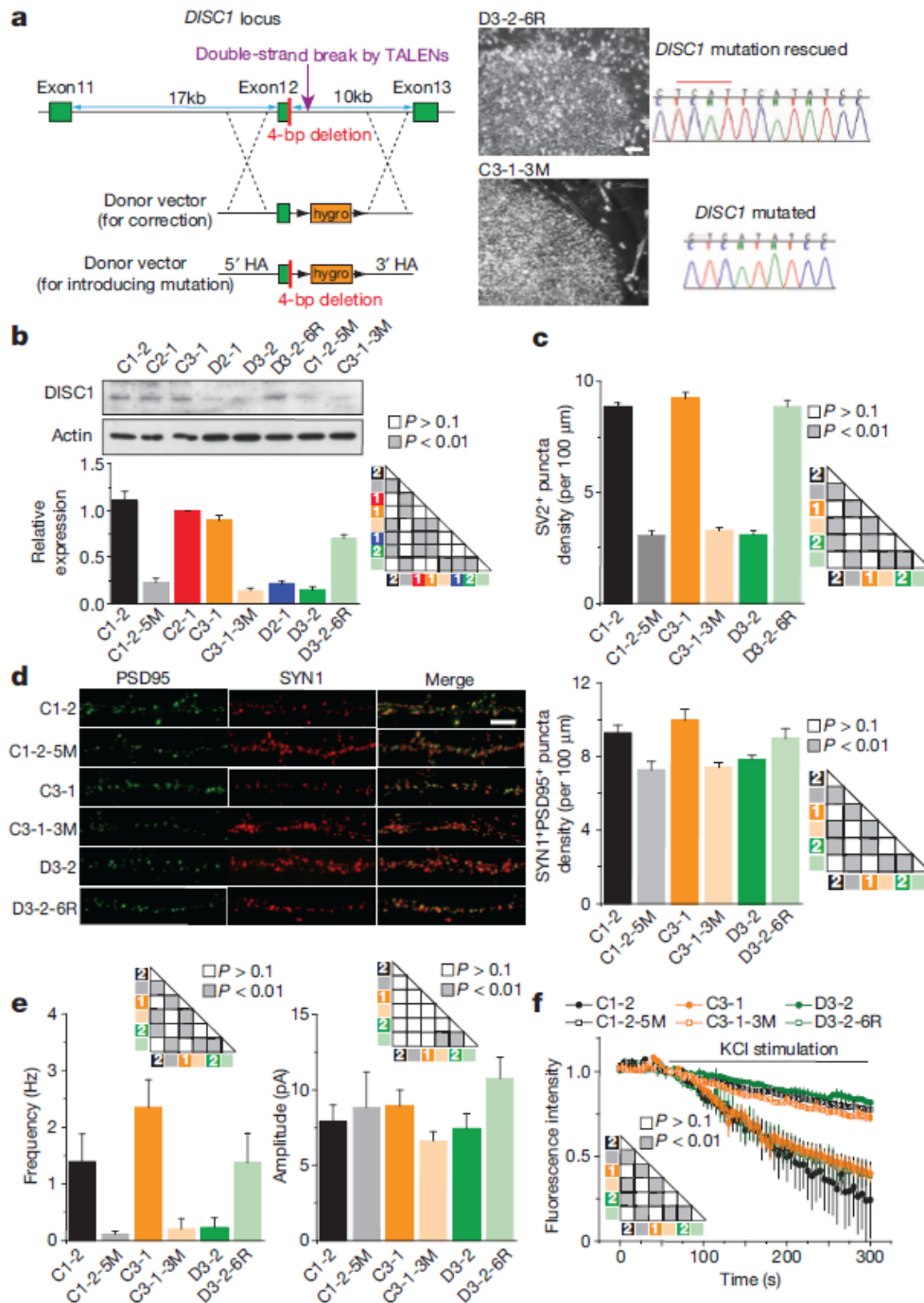FM1-43. Values represent mean ± s.e.m. (n = 4 cultures; ANOVA).

Figure 3. A causal role of the *DISC1* mutation in regulating synapse formation in human forebrain neurons. a, Generation of two types of isogenic iPSC lines. Shown on the left is a schematic illustration of the gene editing strategy for correction of the mutation (4-bp deletion; red bar) in a mutant iPSC line and for knock-in of the same

mutation into two control iPSC lines. HA: homology arm. Shown on the right are sample images of iPSC colonies for the correction line (D3-2-6R) and the knock-in line (C3-1-3M) and confirmation by Sanger sequencing. Scale bar: 50 μm. **b,** Expression of DISC1 protein in forebrain neurons derived from different isogenic iPSC lines. Shown are sample Western blot images and quantification of the total DISC1 protein level. Data were normalized to that of ACTIN for sample loading and then to C2-1 in the same blot for comparison. Values represent mean $\pm$ s.e.m. (n = 3; ANOVA). **c-f,** mDISC1-dependent regulation of synaptic puncta density and vesicle release. Shown in (**d**) are sample confocal images of SYN1 and PSD95 immunostaining. Scale bar: 20 μm. Also shown are summaries of densities of SV2$^+$ puncta (**c**) or SYN1 and PSD95 pair (**d**) of 6 week-old neurons. Values represent mean $\pm$ s.e.m. (n = 4 cultures; ANOVA). Shown in (**e**) are summaries of SSC frequencies and amplitudes. Values represent mean $\pm$ s.e.m. (n = 10-16 neurons for each condition; Kolmogorov–Smirnov test). Shown in (**f**) is a summary of FM1-43 imaging analysis, similarly as in Fig. 2e. Values represent mean $\pm$ s.e.m. (n = 4 cultures; ANOVA).
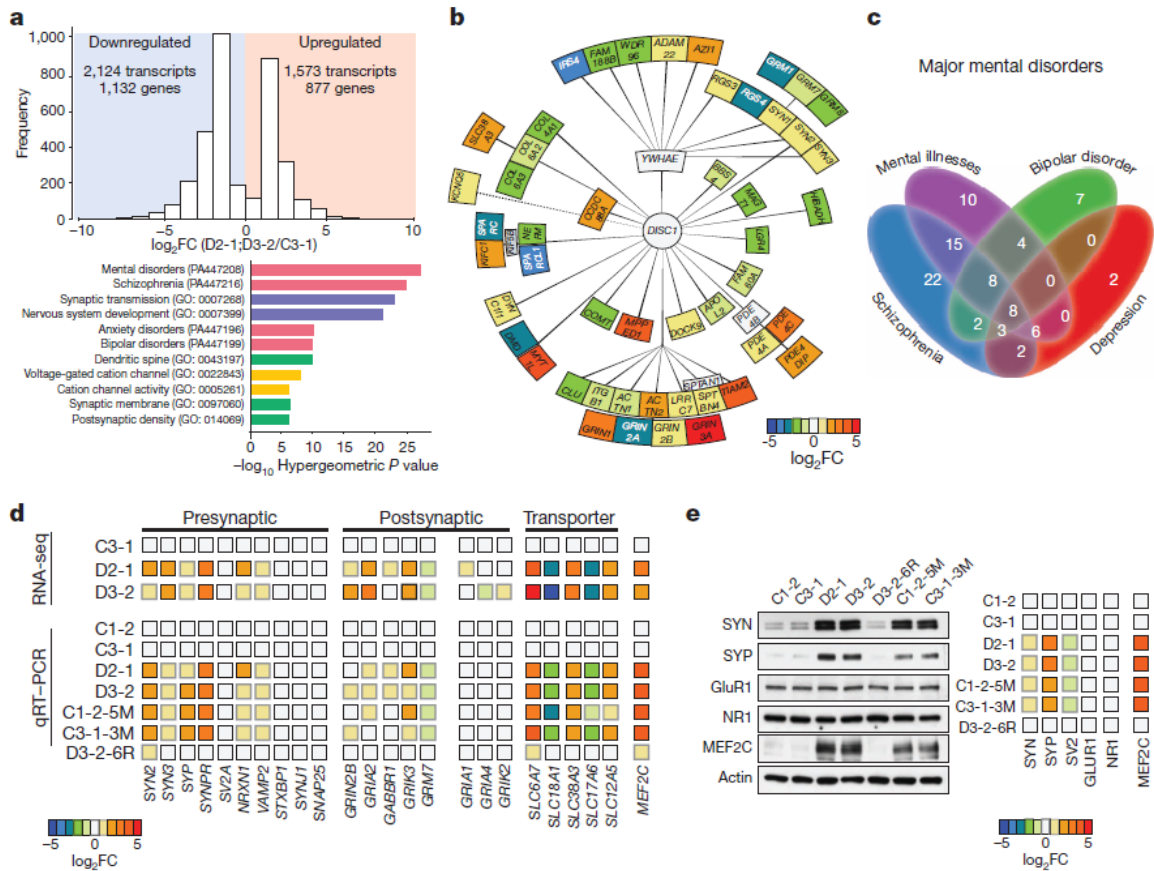
Figure 4. Dysregulation of neuronal transcriptome encoding a subset of presynaptic proteins, DISC1-interacting proteins and mental disorder-associated proteins in human forebrain neurons carrying the *DISC1* mutation. a-c, Summary of RNA-seq analysis of 4-week old forebrain neurons derived from C3-1, D2-1 and D3-2 iPSCs (n = 3 samples for each iPSC line). Shown in (**a**) are histographs of differentially expressed genes in *DISC1* mutant neurons (both D2 and D3) compared to control neurons and GO analysis. Shown in (**b**) is an illustration of differentially expressed genes encoding DISC1-interaction proteins. Heat-map indicates mean values of differential expression for each gene. Shown in (**c**) is an illustration of differentially expressed genes that are related to mental disorders. See Extended Data Table 4e for the gene list. (**d**) Validation of differential mRNA expression of selected genes related to synapses in forebrain neurons from different isogenic iPSC lines. Shown is a heat-map

of mean values of each gene under different conditions (n = 3 experiments). Values

were normalized to those of C3-1 neurons. See Extended Data Fig. 8c for detail. (**e**)

Validation of differential protein expression of selected genes in forebrain neurons from

isogenic iPSC lines. Shown is a heat-map of mean values of each protein under different

conditions (n = 3 experiments). See Extended Data Fig. 8d for detail.

Chapter 4: Conclusions

Cellular reprogramming of patient-derived cells to iPSCs provides a new translational platform for studying human-specific and disease-causing mutations, validating existing hypotheses and generating new hypotheses about psychiatric disease etiology, and uncovering relevant phenotypes and signaling pathways that may be important in the development of more efficacious and targeted therapeutic strategies. Despite the promise of cellular reprogramming technology for all of these purposes, its potential has not been fully realized, yet. The studies highlighted in this dissertation have shown that using iPSCs as a discovery tool can lead to novel biological insights and reveal promising avenues of investigation to understand genetically complex diseases[26]. In the case of 15q11.2 microdeletion, for the first time, a stem cell model served as an entry point to test and to identify a specific risk gene (*CYFIP1*) that affects early brain development in a mouse model and in human large-scale gene expression data sets. And in the other study, for the first time, a *DISC1* frameshift mutation was shown to cause synaptic dysregulation and dysfunction in human forebrain neurons. Together, these studies have enhanced our understanding of the cellular and molecular mechanisms that may contribute to psychiatric disorders, and they have set a new standard for using iPSCs to model disease. However, there are many challenges that must be overcome in order for iPSC technology to be efficiently used to model diseases and to serve as a platform for drug screenings and therapeutics.

A. Major challenges in using iPSCs to model mental disorders

Many diseases affect specific regions or organs in the body and, in particular, psychiatric diseases target the brain. One of the major hurdles in studying psychiatric diseases had

been accessing human neurons. With the advent of iPSC technology, patient-derived neurons generated in the dish provide some remedies[7; 27]. However, the efficiency of differentiating iPSCs into specific neuronal subtypes is still suboptimal[28]. The heterogeneity of different types of neurons at various stages of maturity, and a mixture of different cell types present in the whole population could skew data analysis and make disease phenotypes difficult to observe and validate. To my knowledge, currently, there are no standard protocols that differentiate iPSCs into any pure subtype of neurons. Trying to improve the differentiation efficiency is still an undertaking for many research groups and it remains a struggle in the field.

One way to circumvent the heterogeneity is to use high-throughput next-generation sequencing of single cells to identify the specific neuronal subtypes of interest and their maturation stages and to only compare those with similar identity. This way, any subtle changes in gene expression can be teased out and validated using other methods, such as protein expression analysis and real-time PCR. Although next-generation sequencing is becoming more practical, it is still expensive and the method for analysis is not standardized, yet[29; 30]. Moreover, isolation of single neurons can be challenging and the process may perturb genetic expression.

Another obstacle in using iPSCs to model psychiatric diseases is due to inherent clonal and line-to-line variabilities[31]. In other words, multiple iPSC clones can be derived from one donor (line) and these clones are not identical—they have altered genetics and epigenetics[32]. These changes may influence both the ground state and the disease state of the target cells, which makes comparison between control and disease even more difficult. Also, these clones and lines have different proliferation rates and different propensities to differentiate into neurons. To remedy this problem, prudent stem cell

scientists usually analyze at least two to three iPSC clones from each donor, and when possible, include multiple donors, with their ages matched, into their studies. To make matters even more complicated, not all control lines have similar gene or protein expression levels. This is due to the lines having different genetic backgrounds and to the possibility that not all "control" individuals are completely healthy.

Additionally, with the improvement of genome editing technologies such as CRISPR-cas system and TALENs[33; 34], genetic variability can be overcome by either correcting a disease-causing mutation or introducing a relevant mutation or a reporter into any locus of the genome. Theoretically, this should solve the variability issue; however, manipulation of the genome itself can give rise to off-target effects and risk introducing new mutations that may affect gene activities in the cells[35; 36]. Furthermore, the efficiency of gene editing and homologous recombination are still very low in human iPSCs compared to other cell types[37]. As a result, the screening process, sometimes involving the use of antibiotics, is laborious and it can take up to many months to find the correct clones. During this long period, iPSCs are susceptible to further undersired genetic modifications that may lead to abnormal karyotypes[38].

These challenges I have outlined above are not limited to psychiatric disorders, but they can be extended to other iPSC disease models as well. However, with proper tools to monitor genetic integrity and better differentiation protocols, iPSC technology harnesses tremendous potential in disease modeling and beyond[32; 39].

B. An emerging promise: iPSCs in 3-D modeling

Most iPSC studies have been focused on culture of cells attached to the bottom of the dish in monolayer. Although this two-dimensional system is sufficient to validate some disease phenotypes, it is not ideal to recapitulate some developmental processes that

naturally occur *in vivo* and hallmarks of certain diseases. For example, microcephaly is a neurodevelopmental disorder that affects normal brain development, learning abilities and motor functions[40]. Modeling microcephaly using a two-dimensional system would not be ideal. Recently, Lancaster and co-workers differentiated iPSCs into cerebral organoids that resemble various regions, including the cerebral cortex, of the brain[41]. These organoids were able to grow and develop in three-dimensional suspension in a bioreactor *in vitro*. They further showed that organoids derived from patients with microcephaly not only have premature neuronal differentiation, but are also smaller in size compared to controls. Thus, their findings have paved the way for improvement of the system and for studying diseases that are associated with brain development[42-44]. It is now possible to differentiate human iPSCs into neocortex with primitive cortical layers, similar cellular make-up, and correct organization. With more effort, it is imaginable in the near future that iPSCs can be used to fully model early human brain development—all in 3-D.

References

1. Lieberman, J.A., Stroup, T.S., McEvoy, J.P., Swartz, M.S., Rosenheck, R.A., Perkins, D.O., Keefe, R.S., Davis, S.M., Davis, C.E., Lebowitz, B.D., et al. (2005). Effectiveness of antipsychotic drugs in patients with chronic schizophrenia. The New England journal of medicine 353, 1209-1223.

2. Gupta, S., Ellis, S.E., Ashar, F.N., Moes, A., Bader, J.S., Zhan, J., West, A.B., and Arking, D.E. (2014). Transcriptome analysis reveals dysregulation of innate immune response genes and neuronal activity-dependent genes in autism. Nature communications 5, 5748.

3. De Rubeis, S., He, X., Goldberg, A.P., Poultney, C.S., Samocha, K., Cicek, A.E., Kou, Y., Liu, L., Fromer, M., Walker, S., et al. (2014). Synaptic, transcriptional and chromatin genes disrupted in autism. Nature 515, 209-215.

4. Ripke, S., O'Dushlaine, C., Chambert, K., Moran, J.L., Kahler, A.K., Akterin, S., Bergen, S.E., Collins, A.L., Crowley, J.J., Fromer, M., et al. (2013). Genome-wide association analysis identifies 13 new risk loci for schizophrenia. Nature genetics 45, 1150-1159.

5. Consortium, S.W.G.o.t.P.G. (2014). Biological insights from 108 schizophrenia-associated genetic loci. Nature 511, 421-427.

6. Geschwind, D.H. (2011). Genetics of autism spectrum disorders. Trends in cognitive sciences 15, 409-416.

7. Takahashi, K., Tanabe, K., Ohnuki, M., Narita, M., Ichisaka, T., Tomoda, K., and Yamanaka, S. (2007). Induction of pluripotent stem cells from adult human fibroblasts by defined factors. Cell 131, 861-872.

8. Cherry, A.B., and Daley, G.Q. (2013). Reprogrammed cells for disease modeling and regenerative medicine. Annual review of medicine 64, 277-290.

9. Christian, K., Song, H., and Ming, G.L. (2010). Adult neurogenesis as a cellular model to study schizophrenia. Cell Cycle 9, 636-637.

10. Grskovic, M., Javaherian, A., Strulovici, B., and Daley, G.Q. (2011). Induced pluripotent stem cells--opportunities for disease modelling and drug discovery. Nature reviews Drug discovery 10, 915-929.

11. Brennand, K.J., Simone, A., Jou, J., Gelboin-Burkhart, C., Tran, N., Sangar, S., Li, Y., Mu, Y., Chen, G., Yu, D., et al. (2011). Modelling schizophrenia using human induced pluripotent stem cells. Nature 473, 221-225.

12. Nguyen, H.N., Byers, B., Cord, B., Shcheglovitov, A., Byrne, J., Gujar, P., Kee, K., Schule, B., Dolmetsch, R.E., Langston, W., et al. (2011). LRRK2 Mutant iPSC-Derived DA Neurons Demonstrate Increased Susceptibility to Oxidative Stress. Cell stem cell 8, 267-280.

13. Byers, B., Cord, B., Nguyen, H.N., Schule, B., Fenno, L., Lee, P.C., Deisseroth, K., Langston, J.W., Pera, R.R., and Palmer, T.D. (2011). SNCA triplication Parkinson's patient's iPSC-derived DA neurons accumulate alpha-synuclein and are susceptible to oxidative stress. PLoS ONE 6, e26159.

14. Wen, Z., Nguyen, H.N., Guo, Z., Lalli, M.A., Wang, X., Su, Y., Kim, N.S., Yoon, K.J., Shin, J., Zhang, C., et al. (2014). Synaptic dysregulation in a human iPS cell model of mental disorders. Nature 515, 414-418.

15. Yoon, K.J., Nguyen, H.N., Ursini, G., Zhang, F., Kim, N.S., Wen, Z., Makri, G., Nauen, D., Shin, J.H., Park, Y., et al. (2014). Modeling a genetic risk for schizophrenia in iPSCs and mice reveals neural stem cell deficits associated with adherens junctions and polarity. Cell stem cell 15, 79-91.

16. Burnside, R.D., Pasion, R., Mikhail, F.M., Carroll, A.J., Robin, N.H., Youngs, E.L., Gadi, I.K., Keitges, E., Jaswaney, V.L., Papenhausen, P.R., et al. (2011). Microdeletion/microduplication of proximal 15q11.2 between BP1 and BP2: a susceptibility region for neurological dysfunction including developmental and language delay. Human genetics 130, 517-528.

17. Stefansson, H., Rujescu, D., Cichon, S., Pietilainen, O.P., Ingason, A., Steinberg, S., Fossdal, R., Sigurdsson, E., Sigmundsson, T., Buizer-Voskamp, J.E., et al. (2008). Large recurrent microdeletions associated with schizophrenia. Nature 455, 232-236.

18. Consortium, I.S. (2008). Rare chromosomal deletions and duplications increase risk of schizophrenia. Nature 455, 237-241.

19. Napoli, I., Mercaldo, V., Boyl, P.P., Eleuteri, B., Zalfa, F., De Rubeis, S., Di Marino, D., Mohr, E., Massimi, M., Falconi, M., et al. (2008). The fragile X syndrome protein represses activity-dependent translation through CYFIP1, a new 4E-BP. Cell 134, 1042-1054.

20. Pathania, M., Davenport, E.C., Muir, J., Sheehan, D.F., Lopez-Domenech, G., and Kittler, J.T. (2014). The autism and schizophrenia associated gene CYFIP1 is critical for the maintenance of dendritic complexity and the stabilization of mature spines. Translational psychiatry 4, e374.

21. Doornbos, M., Sikkema-Raddatz, B., Ruijvenkamp, C.A., Dijkhuizen, T., Bijlsma, E.K., Gijsbers, A.C., Hilhorst-Hofstee, Y., Hordijk, R., Verbruggen, K.T., Kerstjens-Frederikse, W.S., et al. (2009). Nine patients with a microdeletion 15q11.2 between breakpoints 1 and 2 of the Prader-Willi critical region, possibly associated with behavioural disturbances. European journal of medical genetics 52, 108-115.

22. Weinberger, D.R. (1987). Implications of normal brain development for the pathogenesis of schizophrenia. Archives of general psychiatry 44, 660-669.

23. Chubb, J.E., Bradshaw, N.J., Soares, D.C., Porteous, D.J., and Millar, J.K. (2008). The DISC locus in psychiatric illness. Molecular psychiatry 13, 36-64.

24. Millar, J.K., Wilson-Annan, J.C., Anderson, S., Christie, S., Taylor, M.S., Semple, C.A., Devon, R.S., St Clair, D.M., Muir, W.J., Blackwood, D.H., et al. (2000). Disruption of two novel genes by a translocation co-segregating with schizophrenia. Human molecular genetics 9, 1415-1423.

25. Sachs, N.A., Sawa, A., Holmes, S.E., Ross, C.A., DeLisi, L.E., and Margolis, R.L. (2005). A frameshift mutation in Disrupted in Schizophrenia 1 in an American family with schizophrenia and schizoaffective disorder. Molecular psychiatry 10, 758-764.

26. Wright, R., Rethelyi, J.M., and Gage, F.H. (2014). Enhancing induced pluripotent stem cell models of schizophrenia. JAMA Psychiatry 71, 334-335.

27. Takahashi, K., and Yamanaka, S. (2006). Induction of pluripotent stem cells from mouse embryonic and adult fibroblast cultures by defined factors. Cell 126, 663-676.

28. Hu, B.Y., Weick, J.P., Yu, J., Ma, L.X., Zhang, X.Q., Thomson, J.A., and Zhang, S.C. (2010). Neural differentiation of human induced pluripotent stem cells follows developmental principles but with variable potency. Proceedings of the National Academy of Sciences of the United States of America 107, 4335-4340.

29. Liu, L., Li, Y., Li, S., Hu, N., He, Y., Pong, R., Lin, D., Lu, L., and Law, M. (2012). Comparison of next-generation sequencing systems. Journal of biomedicine & biotechnology 2012, 251364.

30. Gogol-Doring, A., and Chen, W. (2012). An overview of the analysis of next generation sequencing data. Methods in molecular biology 802, 249-257.

31. Vitale, A.M., Matigian, N.A., Ravishankar, S., Bellette, B., Wood, S.A., Wolvetang, E.J., and Mackay-Sim, A. (2012). Variability in the generation of induced pluripotent

stem cells: importance for disease modeling. Stem cells translational medicine 1, 641-650.

32. Liang, G., and Zhang, Y. (2013). Genetic and epigenetic variations in iPSCs: potential causes and implications for application. Cell stem cell 13, 149-159.

33. Sander, J.D., and Joung, J.K. (2014). CRISPR-Cas systems for editing, regulating and targeting genomes. Nature biotechnology 32, 347-355.

34. Joung, J.K., and Sander, J.D. (2013). TALENs: a widely applicable technology for targeted genome editing. Nature reviews 14, 49-55.

35. Cho, S.W., Kim, S., Kim, Y., Kweon, J., Kim, H.S., Bae, S., and Kim, J.S. (2014). Analysis of off-target effects of CRISPR/Cas-derived RNA-guided endonucleases and nickases. Genome research 24, 132-141.

36. Wang, X., Wang, Y., Wu, X., Wang, J., Wang, Y., Qiu, Z., Chang, T., Huang, H., Lin, R.J., and Yee, J.K. (2015). Unbiased detection of off-target cleavage by CRISPR-Cas9 and TALENs using integrase-defective lentiviral vectors. Nature biotechnology 33, 175-178.

37. Aizawa, E., Hirabayashi, Y., Iwanaga, Y., Suzuki, K., Sakurai, K., Shimoji, M., Aiba, K., Wada, T., Tooi, N., Kawase, E., et al. (2012). Efficient and accurate homologous recombination in hESCs and hiPSCs using helper-dependent adenoviral vectors. Molecular therapy : the journal of the American Society of Gene Therapy 20, 424-431.

38. Peterson, S.E., and Loring, J.F. (2014). Genomic instability in pluripotent stem cells: implications for clinical applications. The Journal of biological chemistry 289, 4578-4584.

39. Okita, K., and Yamanaka, S. (2011). Induced pluripotent stem cells: opportunities and challenges. Philosophical transactions of the Royal Society of London Series B, Biological sciences 366, 2198-2207.

40. Woods, C.G., Bond, J., and Enard, W. (2005). Autosomal recessive primary microcephaly (MCPH): a review of clinical, molecular, and evolutionary findings. American journal of human genetics 76, 717-728.

41. Lancaster, M.A., Renner, M., Martin, C.A., Wenzel, D., Bicknell, L.S., Hurles, M.E., Homfray, T., Penninger, J.M., Jackson, A.P., and Knoblich, J.A. (2013). Cerebral organoids model human brain development and microcephaly. Nature 501, 373-379.

42. Mariani, J., Coppola, G., Zhang, P., Abyzov, A., Provini, L., Tomasini, L., Amenduni, M., Szekely, A., Palejev, D., Wilson, M., et al. (2015). FOXG1-Dependent Dysregulation of GABA/Glutamate Neuron Differentiation in Autism Spectrum Disorders. Cell 162, 375-390.

43. Pasca, A.M., Sloan, S.A., Clarke, L.E., Tian, Y., Makinson, C.D., Huber, N., Kim, C.H., Park, J.Y., O'Rourke, N.A., Nguyen, K.D., et al. (2015). Functional cortical neurons and astrocytes from human pluripotent stem cells in 3D culture. Nature methods 12, 671-678.

44. Kadoshima, T., Sakaguchi, H., Nakano, T., Soen, M., Ando, S., Eiraku, M., and Sasai, Y. (2013). Self-organization of axial polarity, inside-out layer pattern, and species-specific progenitor dynamics in human ES cell-derived neocortex. Proceedings of the National Academy of Sciences of the United States of America 110, 20284-20289.

Curriculum Vitae

Contact information

Name: Ha Nam Nguyen
Address: 733 N. Broadway, MRB 706, Baltimore, MD 21205
Work phone: (443) 287-5607(8)
Mobile phone: (415) 713-3195
Email: nam@jhmi.edu

Education

2002	B.S., Cell and Molecular Biology, San Francisco State University
2006	M.S. Cell and Molecular Biology, San Francisco State University (with Wilfred Denetclaw, Jr., Ph.D.)
2015 (Exp.)	Ph.D., Cellular and Molecular Medicine, Johns Hopkins University School of Medicine (with Hongjun Song, Ph.D.)

Research and professional experience

2001-2002	Undergraduate Researcher, Department of Biology, San Francisco State University (with Wilfred Denetclaw, Jr., Ph.D.)
2004-2007	Staff Research Associate II, Department of Obstetrics, Gynecology and Reproductive Sciences, University of California, San Francisco (with Renee Reijo Pera, Ph.D.)
2005-2007	Medical Interpreter, Lan Do & Associates, San Francisco
2007-2010	Research Training Specialist, Institute for Stem Cell Biology and Regenerative Medicine, Stanford University (with Renee Reijo Pera, Ph.D.)

Honors and awards

2001	Dean's List, San Francisco State University
2002	College of Science and Engineering 4th Annual Student Showcase & Alumni Reception, Undergraduate-level Poster Award, San Francisco State University
2013-2015	Ruth L. Kirschstein National Research Service Award for Predoctoral Fellowship, F31, NIMH
2015	Selected as a participant in the 14th Annual National Graduate Student Symposium, St. Jude Children's Research Hospital
2015	Paul Ehrlich Research Award, 38th Annual Young Investigators' Day, Johns Hopkins University School of Medicine

Publications (In reverse chronological order, * Equal contribution)

1. Wen, Z.*, **Nguyen, H.N.*,** Guo, Z.*, Lalli, M.A., Wang, X., Su, Y., Kim, N.S., Yoon, K.J., Shin, J., Zhang, C., Markri, G., Nauen, D., Yu, H., Guzman, E., Chiang, C.H., Yoritomo, N., Kaibuchi, K., Zou, J., Christian, K.M., Cheng, L., Ross, C.A., Margolis, R., Chen, G., Kosik, K.S., Song, H, Ming, G.L. (2014). Synaptic dysregulation in a human iPSC model of mental disorders. *Nature* 515, 414-418.

2. Yoon, K.J., **Nguyen, H.N.**, Ursini, G., Zhang, F., Kim, N.S., Wen, Z., Makri, G., Shin, J.H., Park, Y., Chung, R. Pekle, E., Zhang, C., Towe, M., Hussani, Q., Lee, Y., Rujescu, D., St Clair, D., Kleinman, J.E., Hyde, T.M., Krauss, G., Christian, K.M., Rapoport, J.L, Weinberger, D.R., Song, H., and Ming, G.L. (2014). Mental disorder risk gene CYFIP1 maintains adherens junctions and polarity of human and mouse cortical neural stem cells. *Cell Stem Cell* 15, 79-91.

3. Hu, S., Wan, J., Su, Y., Song, Q., Zeng, Y., **Nguyen, H.N.**, Shin, J., Cox, E., Rho, H.S., Woodard, C., Xia, S., Ming, G.L., Wade, H., Song, H., Qian, J., and Zhu, H. (2013). DNA methylation presents distinct binding sites for human transcription factors. *eLife* 2, e00726.

4. Weier, J.F.*, Hartshorne, C.*, **Nguyen H.N.***, Baumgartner, A., Polyzos A.A., Lembke, K.H., Zeng, H., and Weier, H.U. (2013). Analysis of human invasive cytotrophoblasts using multicolor fluorescence in situ hybridization. *Methods* 64, 160-168.

5. Medrano, J.V., Ramathal, C., **Nguyen, H.N.**, Simon, C., and Reijo-Pera, R.A. (2012). Divergent RNA-binding proteins, DAZL and VASA, induce meiotic progression in human germ cells derived *in vitro*. *Stem Cells* 30, 441-51.

6. Byers, B.*, Cord, B,*, **Nguyen, H.N.***, Schüle, B., Fenno, L., Lee, P.C., Deisseroth, K., Langston, J.W., Reijo Pera, R., and Palmer, T.D. (2011). SNCA Triplication Parkinson's Patient's iPSC-derived DA Neurons Accumulate α-Synuclein and Are Susceptible to Oxidative Stress. *PLoS One* 6, e26159.

7. Rufaihah A.J., Huang N.F., Jame S., Lee J., **Nguyen H.N.**, Byers B., De A., Okogbaa J., Rollins M., Reijo-Pera R., Gambhir S.S., and Cooke J.P. (2011). Endothelial cells derived from human iPSCs increase capillary density and improve perfusion in a mouse model of peripheral arterial disease. *Arterioscler Thromb Vasc Biol.* 31, e72-e79.

8. Batista, L. F., Pech, M. F., Zhong, F. L., **Nguyen, H. N.**, Xie, K. T., Zaug, A. J., Crary, S. M., Choi, J., Sebastiano, V., Cherry, A., Giri, N., Wernig, M., Alter, B. P., Cech, T. R., Savage, S. A., Reijo Pera, R. A., and Artandi, S. E. (2011). Telomere shortening and loss of self-renewal in dyskeratosis congenita induced pluripotent stem cells. *Nature* 474, 399-402.

9. **Nguyen, H.N.***, Byers, B.*, Cord, B.*, Shcheglovitov, A., Byrne, J., Gujar, P., Kee, K., Schüle, B., Dolmetsch, R.E., Langston, W., Palmer, T.D., and Reijo Pera, R (2011). Lrrk2 mutant ipsc-derived DA neurons demonstrate increased susceptibility to oxidative stress. *Cell Stem Cell* 8, 267-280.

10. Panula, S., Medrano, J.V., Kee, K., Bergstrom, R., **Nguyen, H.N.**, Byers, B., Wilson, K.D., Wu, J.C., Simon, C., Hovatta, O., and Reijo Pera, R.A. (2011). Human germ cell differentiation from fetal- and adult-derived induced pluripotent stem cells. *Hum Mol Genet.* 20, 752-762.

11. Kee K., Angeles V.T., Flores M., **Nguyen H.N.**, Reijo Pera R.A (2009). Human *DAZL, DAZ* and *BOULE* genes modulate primordial germ cell and haploid gamete formation. *Nature* 462, 222-225.

12. Byrne, J.A., **Nguyen, H.N.**, and Reijo Pera, R.A. (2009). Enhanced generation of induced pluripotent stem cells from a subpopulation of human fibroblasts. *PLoS One* 4, e7118.

13. Kossack, N., Meneses, J., Shefi, S., **Nguyen, H.N.**, Chavez, S., Nicholas, C., Gromoll, J., Turek, P.J., and Reijo-Pera, R.A. (2009). Isolation and characterization of pluripotent human spermatogonial stem cell-derived cells. *Stem Cells* 27, 138-149.

14. Chavez, S.L., Meneses, J.J., **Nguyen, H.N.,** Kim, S.K., and Pera, R.A. (2008). Characterization of Six New Human Embryonic Stem Cell Lines (HSF7, -8, -9, -10, -12, and -13) Derived Under Minimal-Animal Component Conditions. *Stem Cells and Dev.* 17, 535-546.

15. **Nguyen, H.N.** and Reijo Pera, R.A. (2008). Metaphase Spreads and Spectral Karyotyping of Human Embryonic Stem Cells. *CSH Protocols* doi:10.1101/pdb.prot5047.

16. Privette, L.M., Weier, J.F., **Nguyen, H.N.,** Yu, X., and Petty, E.M. (2008). Loss of CHFR in human mammary epithelial cells causes genomic instability by disrupting the mitotic spindle assembly checkpoint. *Neoplasia* 10, 643-652.

17. Weier, J.F., Ferlatte, C., Baumgartner, A., Jung, C.J., **Nguyen, H.N.,** Chu, L.W., Pedersen, R.A., Fisher, S.J., and Weier, H.U. (2006). Molecular cytogenetic studies towards the full karyotype analysis of human blastocysts and cytotrophoblasts. *Cytogenet Genome Res.* 114, 302-311.

Meeting Abstracts

1. **Nguyen, H.N.**, Wen, Z., Yoon, K.J., Ming, G.L., and Song, H. (2015). Modeling mental disorders using patient-derived induced pluripotent stem cells. National Graduate Student Symposium, St. Jude Children's Research Hospital, Memphis, TN.

2. **Nguyen, H.N.**, Byers, B.H., Byrne, J., Chiao, E., Kee, K., and Reijo Pera, R. (2008). Characterization of induced pluripotent stem cells derived from human adult skin fibroblasts. Germ Cell Meeting, Cold Spring Harbor Laboratory, NY.

3. **Nguyen, H.N.** and Denetclaw, W.F., Jr. (2004). Early myotome formation in the central dermomyotome shows progressive medio-lateral development along cranial and caudal lips and in ectopically formed lips in chicken embryos. Society for Developmental Biology 63rd Annual Meeting, Alberta, Canada.

4. **Nguyen, H.N.** and Denetclaw, W.F., Jr. (2003). The fate of the Kaehn fibers during early epaxial myotome formation in the chicken embryos. Experimental Biology, San Diego, CA.

5. **Nguyen, H.N.**, Godinez, G., and Denetclaw, W.F., Jr. (2002). The fate of the Kaehn fibers during early epaxial myotome formation in chicken embryos. American Society for Cell Biology, 42nd Annual Meeting, San Francisco, CA.

Teaching experience

2002, Fall   **Teaching Assistant**, Cell Biology, Department of Biology, San Francisco State University

2003, Spring	**Teaching Assistant**, Experimental in Cell & Molecular Biology, Department of Biology, San Francisco State University
2003, Fall	**Graduate Teaching Assistant**, Human Biology Laboratory, Department of Biology, San Francisco State University
2007-2010	**Instructor**, Human Pluripotent Stem Cell Laboratory Course, Institute for Stem Cell Biology and Regenerative Medicine, Stanford University
2008-2010	**Advisor**, Institute for Stem Cell Biology and Regenerative Medicine, Stanford University. Mentored Prachi Gujar, a Master's graduate student from San Jose State University.
2013, Spring	**Teaching Assistant**, Stem Cells: Unit of Development and Unit of Regeneration, Department of Neuroscience, Johns Hopkins University School of Medicine
2013-present	**Advisor**, Institute for Cell Engineering, Johns Hopkins University School of Medicine. Mentored undergraduate students: Jai Thakor (Provost's Undergraduate Research Award, 2014) and Michael Chickering (PURA, 2015); and high school students: Chris Hadiono (2015 Neuroscience Research Prize Finalist), Mingxi Song, and William Jeang

Community service

2010 – 2014	Mentor, Thread (Incentive Mentoring Program), Baltimore, MD.